Latest Higgs Inclusive and Differential Cross-Section Measurements

Robin Hayes

Moriond EW
March 28, 2025

ATLAS EXPERIMENT

UNIVERSITY OF AMSTERDAM

Nikhef

Introduction

From Discovery to Today

- We have been studying the Higgs boson since its discovery at the Large Hadron Collider (LHC) in 2012.
- Lots of progress in characterizing it… but there's still more to learn.

This talk:

- New results for Moriond from the ATLAS and CMS experiments, covering measurements of Higgs boson cross-sections.

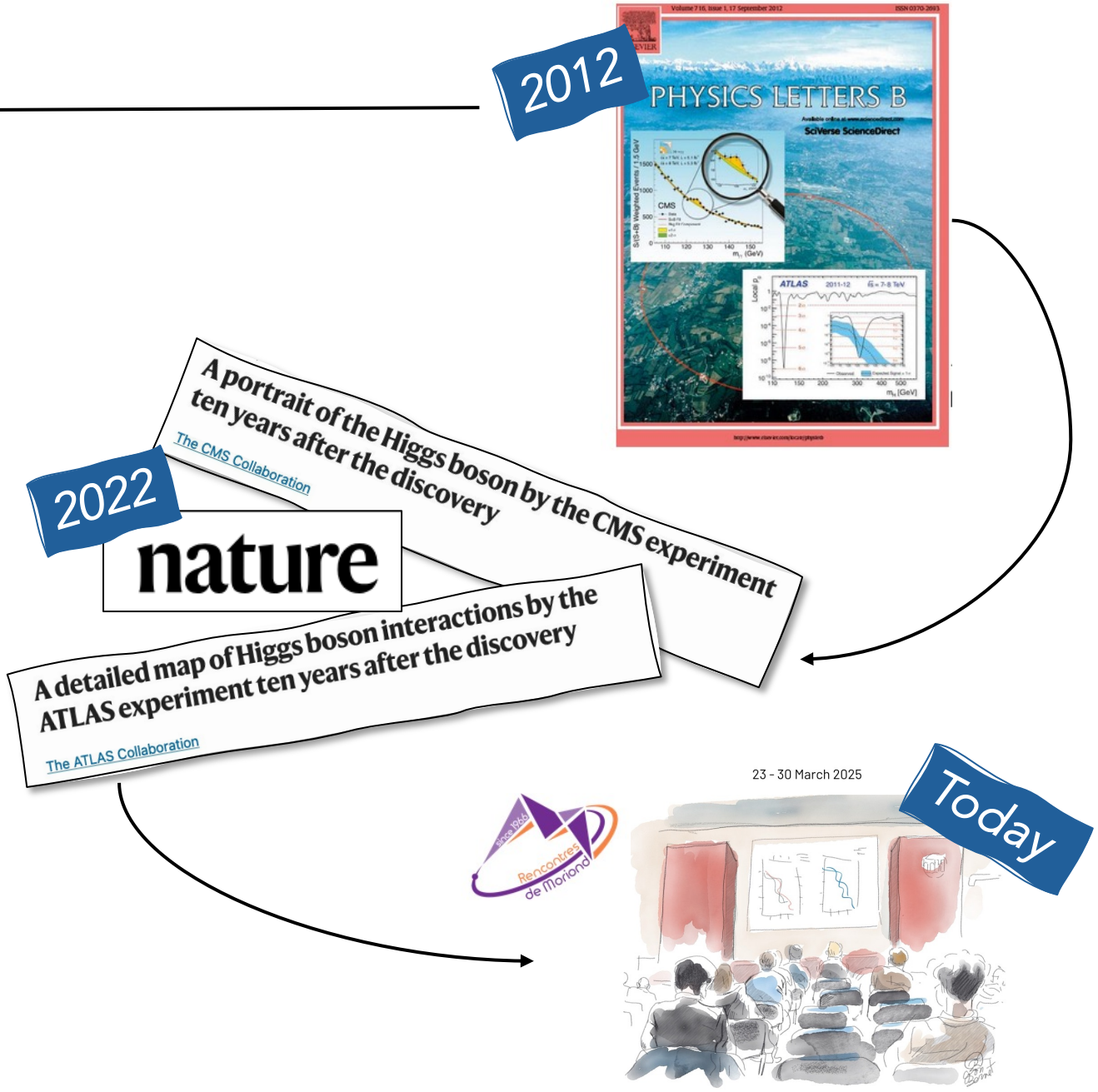

Cross-Section Measurements at the LHC

The measurements discussed today cover a selection of the main production modes at the LHC:

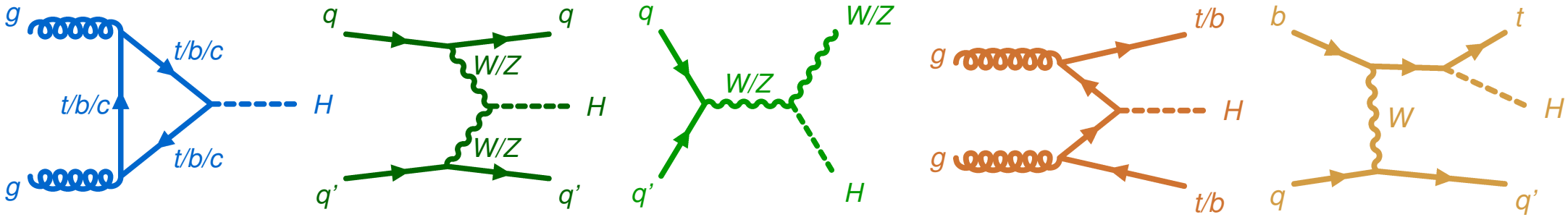

Gluon fusion (ggF) (87%)

Vector boson fusion (VBF) (7%)

Vector boson associated production (VH) (4%)

Top- and bottom-associated production, single-top production (2%)

Cross-Section Measurements at the LHC

The measurements discussed today cover a selection of the main production modes at the LHC:

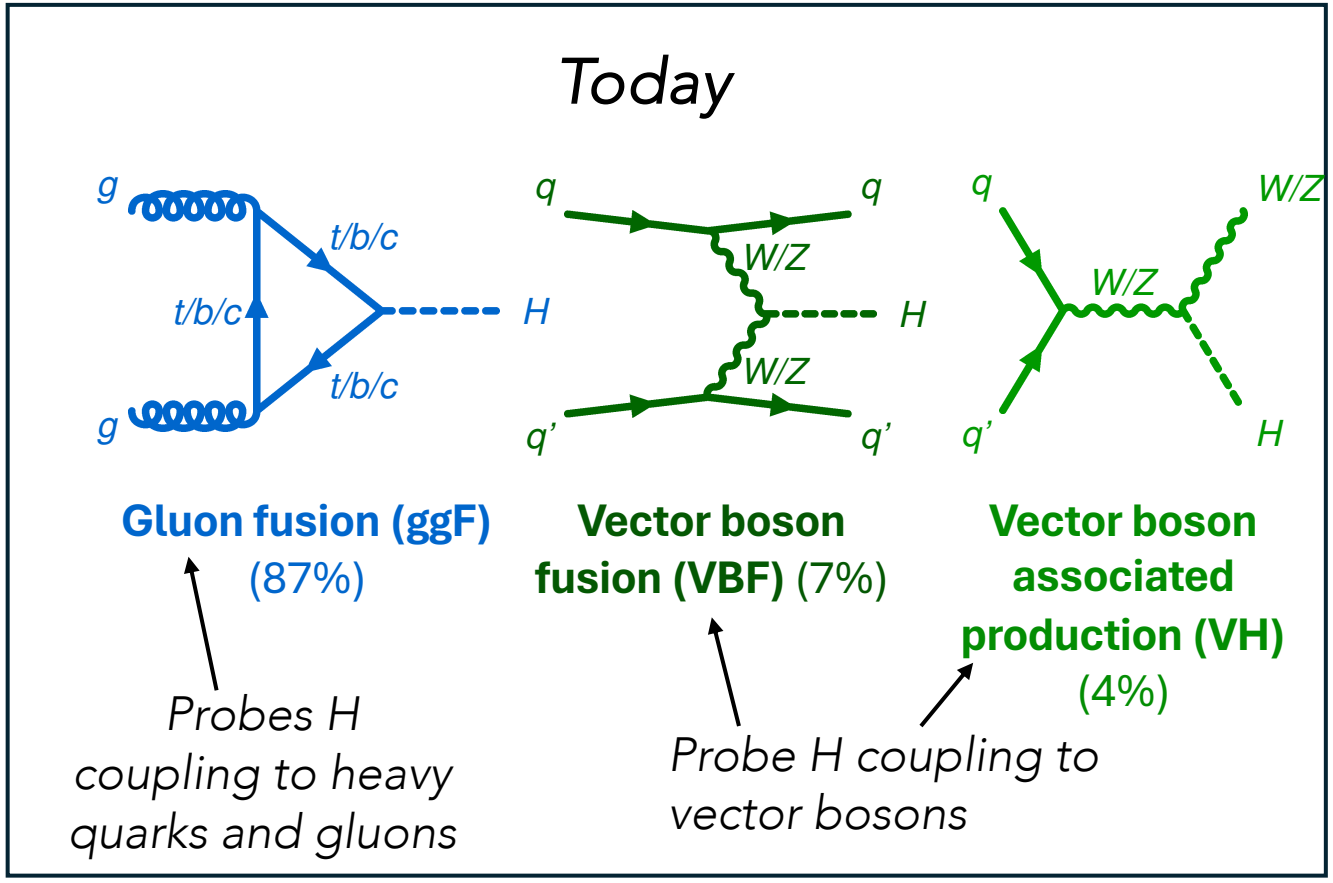

Cross-Section Measurements at the LHC

So far: all consistent with the Standard Model (SM):

eg. CMS [Nature, 2022]:

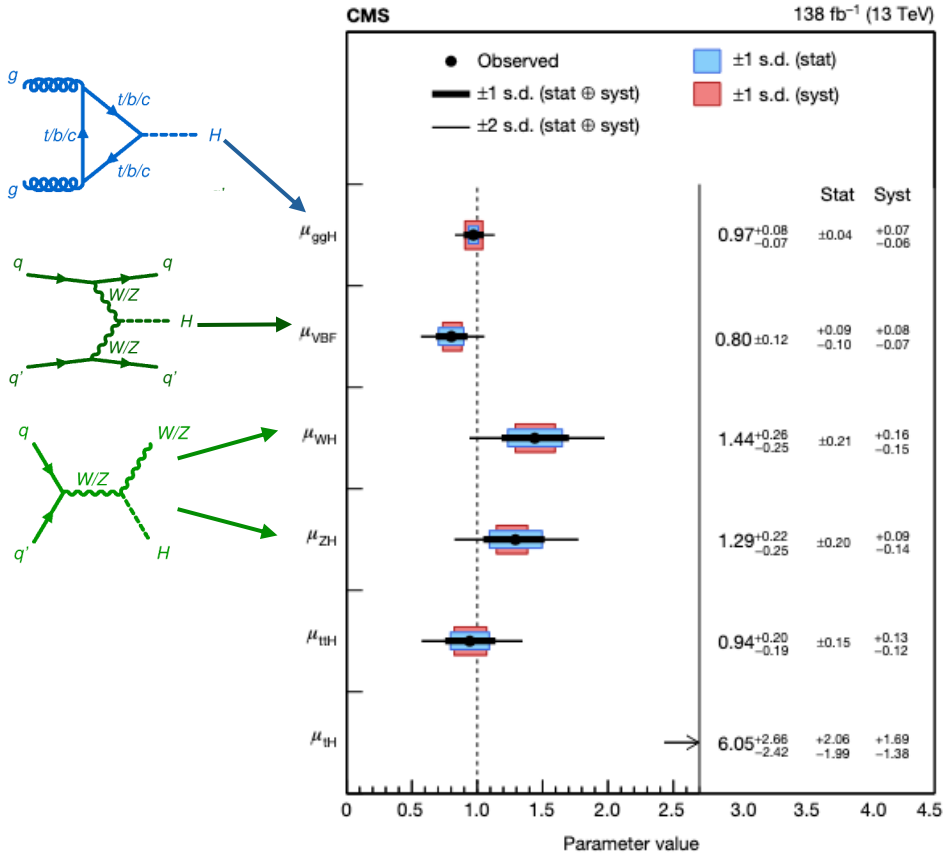

.... But the analyses covered today try to go further in some way:

- ✓ Covering the *boosted* (high-p_T^H) phase space
- ✓ Investigating granular kinematic regions via *Simplified Template Cross-Sections* (STXS)

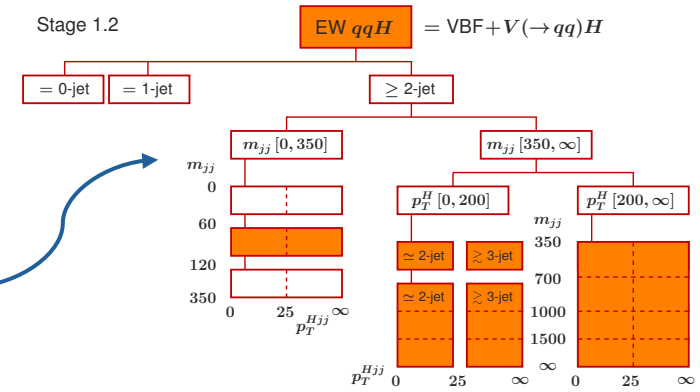

- ✓ Probing for physics beyond our current direct energy reach using *Effective Field Theory* (EFT)

Recent Cross-Section Measurements

The results presented here join many xsec measurements released in the past year:

ATLAS VH $H \to bb/cc$ [HIGG-2020-020]

ATLAS $H \to \tau\tau$ [HIGG-2022-07]

ATLAS $t\bar{t}H$ $H \to bb$ [HIGG-2020-24]

Dec. 2024!

CMS $t\bar{t}H$ $H \to WW/\tau\tau$ [HIG-23-015]

CMS $t\bar{t}H$ and tH $H \to bb$ [HIG-19-011]

CMS boosted ggF and VBF $H \to bb$ [HIG-21-020]

CMS boosted $H \to \tau\tau$ [HIG-21-017]

CMS diff xsec combo [HIG-23-013]

Jan. 2025!

CMS $H \to ZZ$ fid and diff xsec [HIG-24-013]

Run 2 (13 TeV)
Run 3 (13.6 TeV)

New Results for Moriond

Boosted $H \to b\bar{b}$

- $H \to b\bar{b}$: largest branching ratio, allows probing extreme regions of phase space.
  - eg. high-p_{T}^{H} regime: BSM physics effects may be enhanced

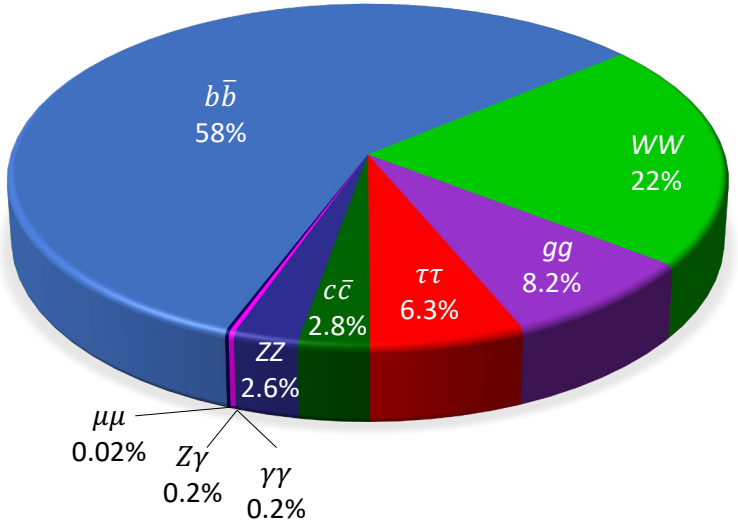

- $b\bar{b}$ decays mainly reconstructed as single large-R jet:

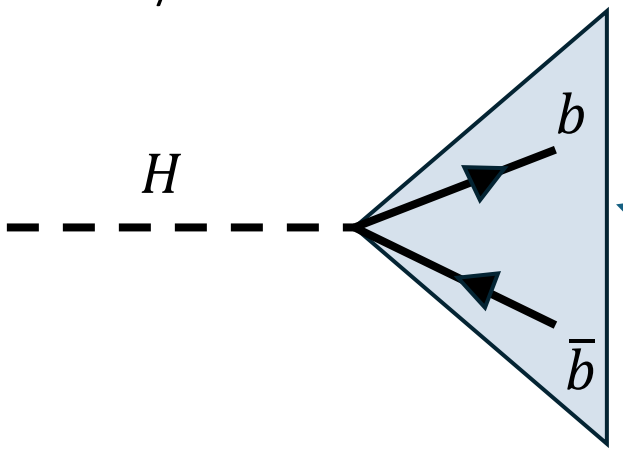

collimated bb pair → merge into one large-R jet (CMS: R=0.8).

- Previous Run 2 measurements studying boosted regime with $H \to b\bar{b}$ decays: CMS ggF + VBF $H \to b\bar{b}$, CMS V(lep) $H \to bb$, ATLAS V(lep)H $H \to bb/cc$, ATLAS V(qq) $H \to bb$, ATLAS incl. $H \to bb$.

New for Moriond: CMS Run 2 boosted $V(qq)H(\to b\bar{b})$.

Boosted V(qq)H(bb)

CMS-PAS-HIG-24-017 (link not public yet)

Strategy:

- Use ParticleNet-MD: mass-decorrelated, GNN-based tagger for 2-prong hadronic decays.
- $V \to qq$ and $H \to bb$ candidates identified with ParticleNet-MD discriminants
- Events classified by V-candidate mass and ParticleNet-MD *Xbb* discriminant score.

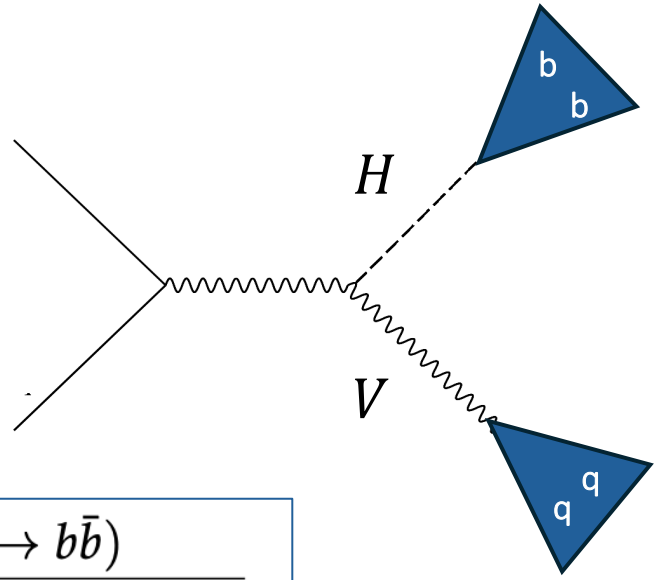

$$\frac{p(X \to b\bar{b})}{p(X \to b\bar{b}) + p(\mathrm{QCD})}.$$

Defines ParticleNet-MD Xbb pass/fail regions

Backgrounds:

- Data-driven estimate of QCD bkg, using events that fail ParticleNet-MD *Xbb* tagger requirement.
- Top quark bkg modelled with MC; normalization set in Top CR
- *W*-enriched CR to calibrate ParticleNet-MD efficiency and derive jet mass scale and resolution scale factors.

Boosted V(qq)H(bb)

CMS-PAS-HIG-24-017 (link not public yet)

Jet mass after soft-drop grooming (reduces underlying event and pileup contamination)

Results:

- Fit to m_{SD} distribution performed across CRs and SRs (including V-mass sidebands)
- Signal strengths and significances measured for $V(qq)H(bb)$ and $V(qq)Z(bb)$ processes:

$$\mu_{VH} = 0.72^{+0.75}_{-0.71}, \quad Z_0 = 1.00(1.64)\sigma \text{ obs(exp)}$$

$$\mu_{VZ} = 0.09^{+0.63}_{-0.63}, \quad Z_0 = 0.15(1.76)\sigma \text{ obs(exp)}$$

ParticleNet-MD Xbb Pass region, with other jet in V-mass window.

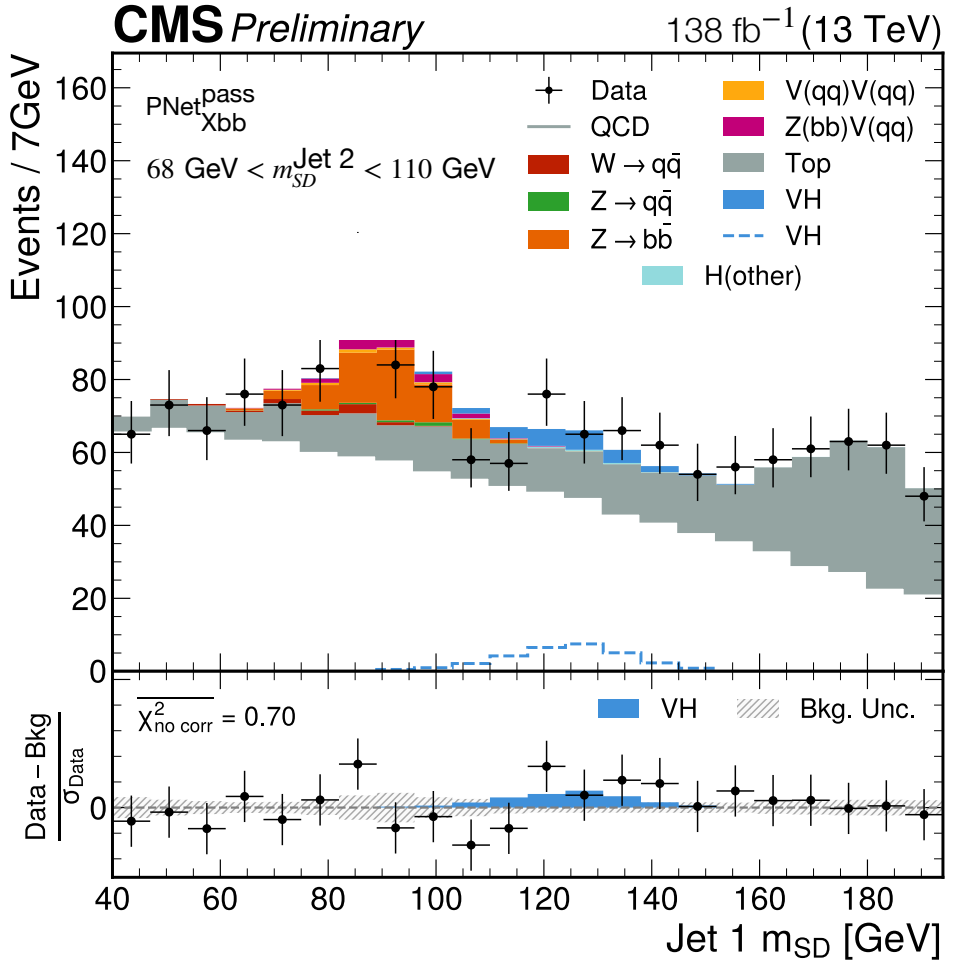

ggF, VBF and VH $H \rightarrow WW^*$

- $H \rightarrow WW^*$: second-largest branching ratio, clean $WW^* \rightarrow \ell\nu\ell\nu$ decay mode
  - Probes Higgs boson coupling to vector bosons.

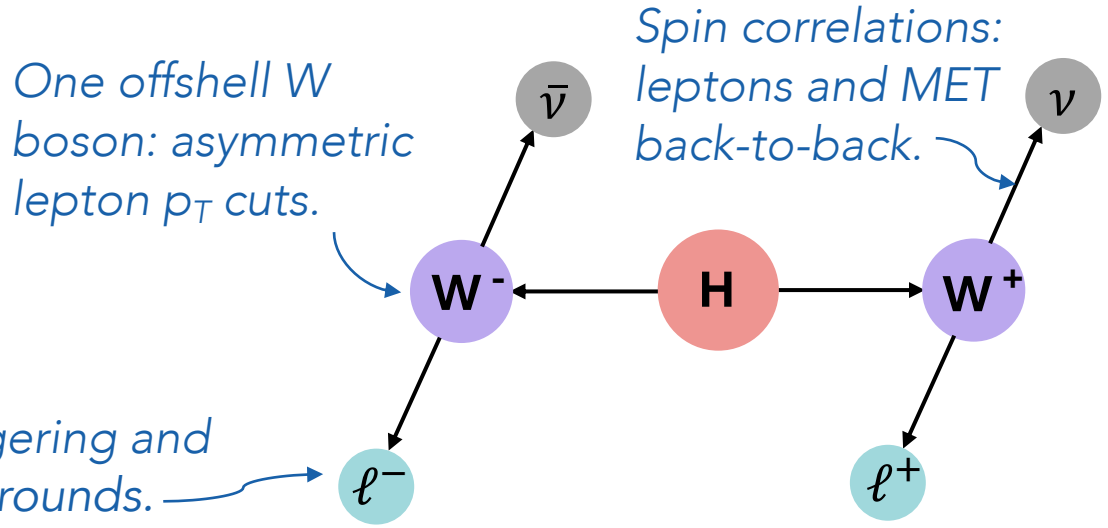

New for Moriond: ATLAS 13 TeV measurements in the $H \rightarrow WW^*$ channel:

- ggF and VBF signal strengths, cross-sections, STXS, and EFT interpretation [update of first Full Run 2 paper]
- WH and ZH signal strengths, cross-sections, STXS [update of preliminary result]

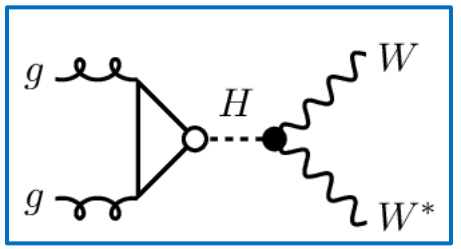

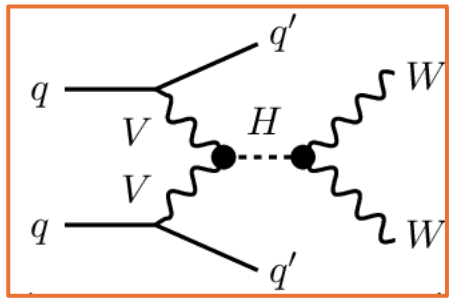

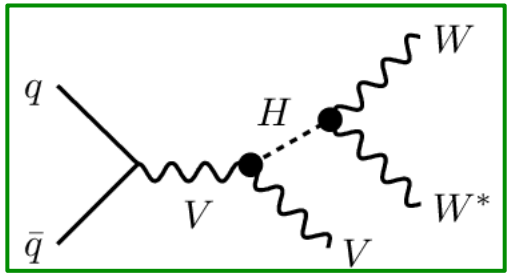

ggF and VBF $H \rightarrow WW^*$

CERN-EP-2025-054

Strategy:

- Target ggF and VBF STXS Stage 1.2 bins
- Different-flavour (DF, $e\nu\mu\nu$) and same-flavour (SF $e\nu e\nu / \mu\nu\mu\nu$) final states
- Categorize events by production mode, SF/DF, $p_{\mathrm{T}}^{H}, m_{jj}, N_{\mathrm{jets}}$ → 22 signal regions.
- Multiple improvements since previous analysis:
  - Use of SF channel in stats-limited high-p_T^H regions
  - DNNs as final discriminants
  - Better lepton isolation → smaller misID lepton background.

DF SRs covering highest-p_T^H VBF bins

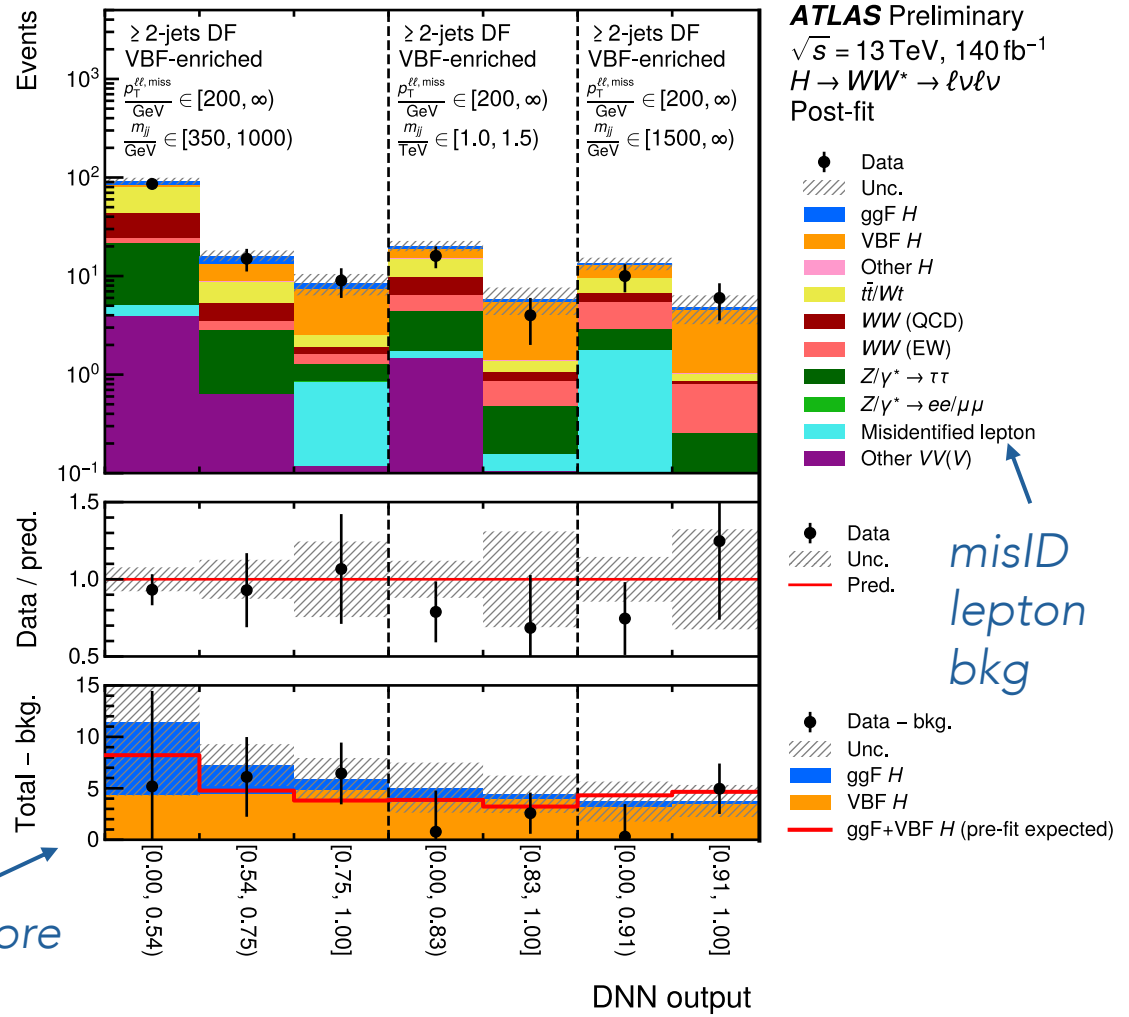

bins of DNN score

misID lepton bkg

ggF and VBF $H \rightarrow WW^*$

CERN-EP-2025-054

Results:

- Measure σ_{ggF} and σ_{VBF}, and STXS cross-sections
- Compared to first 13 TeV paper:
  - 11% more precise for σ_{ggF} and σ_{VBF}.

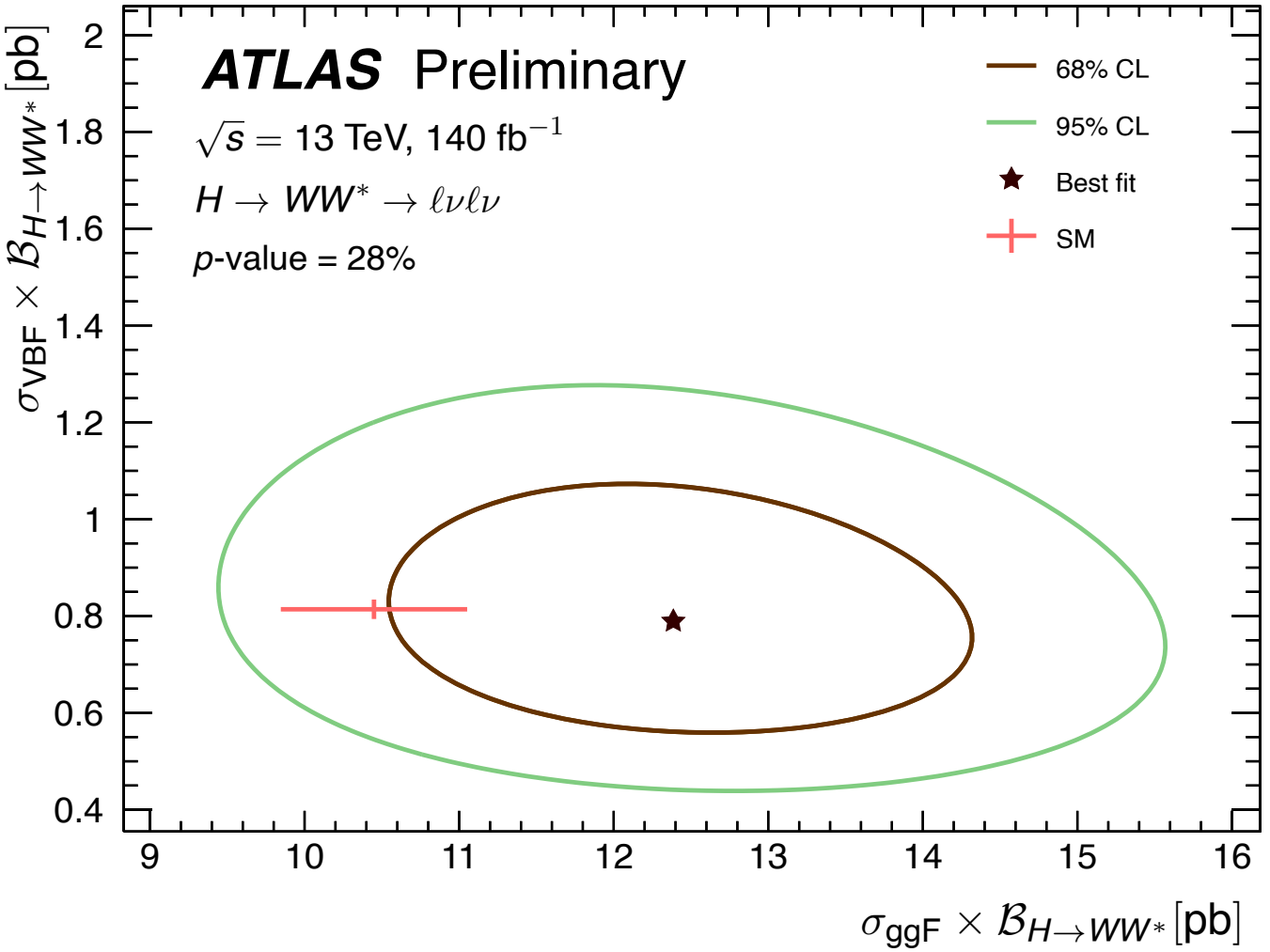

ggF and VBF $H \rightarrow WW^*$

CERN-EP-2025-054

Results:

- Measure σ_{ggF} and σ_{VBF}, and STXS cross-sections
- Compared to first 13 TeV paper:
  - 11% more precise for σ_{ggF} and σ_{VBF}.
  - 15 STXS categories resolved (11 last time).

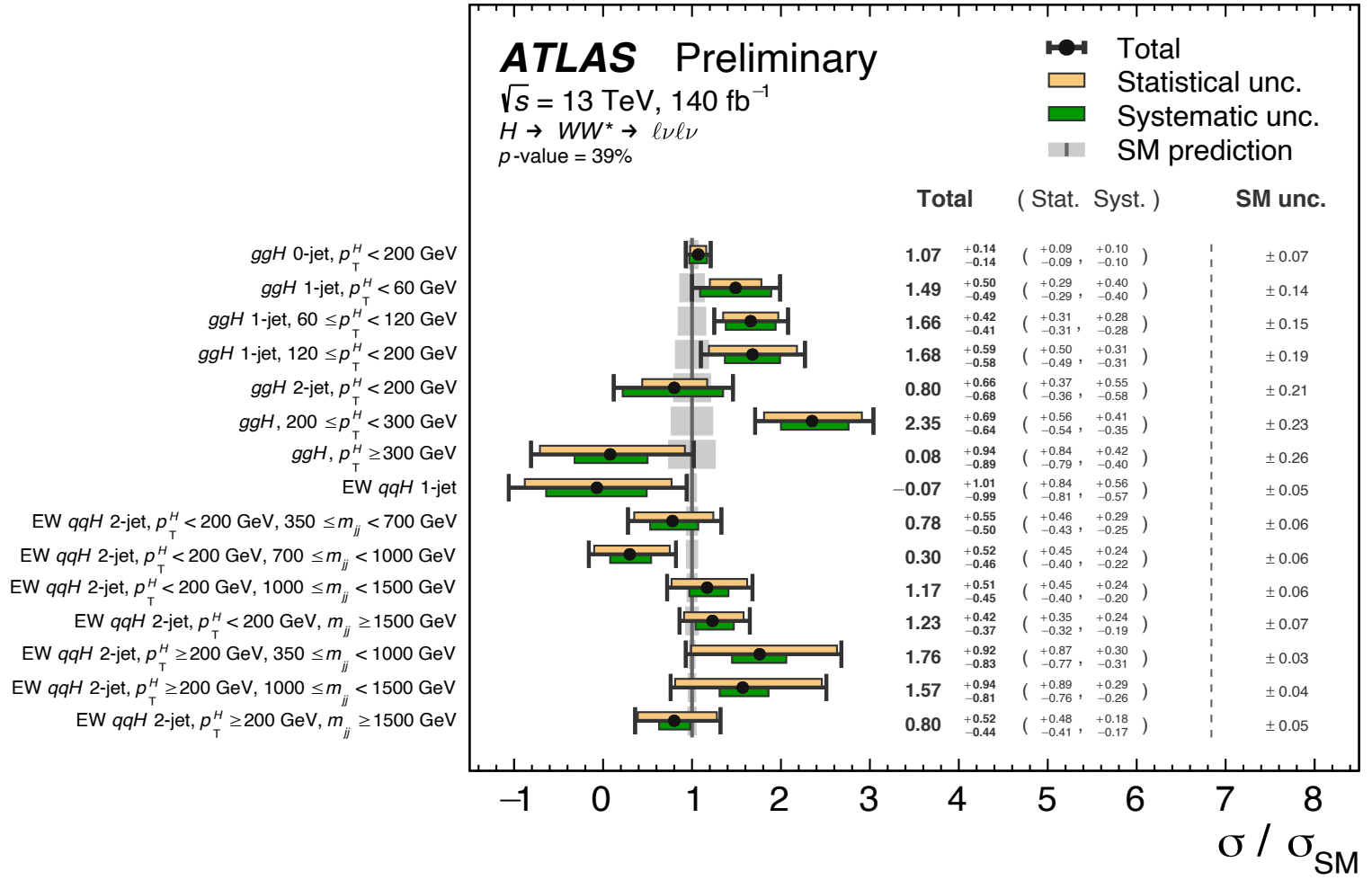

ggF and VBF $H \rightarrow WW^*$

CERN-EP-2025-054

Results:

- Measure σ_{ggF} and σ_{VBF}, and STXS cross-sections
- Compared to first 13 TeV paper:
  - 11% more precise for σ_{ggF} and σ_{VBF}.
  - 15 STXS categories resolved (11 last time)
  - 10-20% more precise for VBF STXS categories.

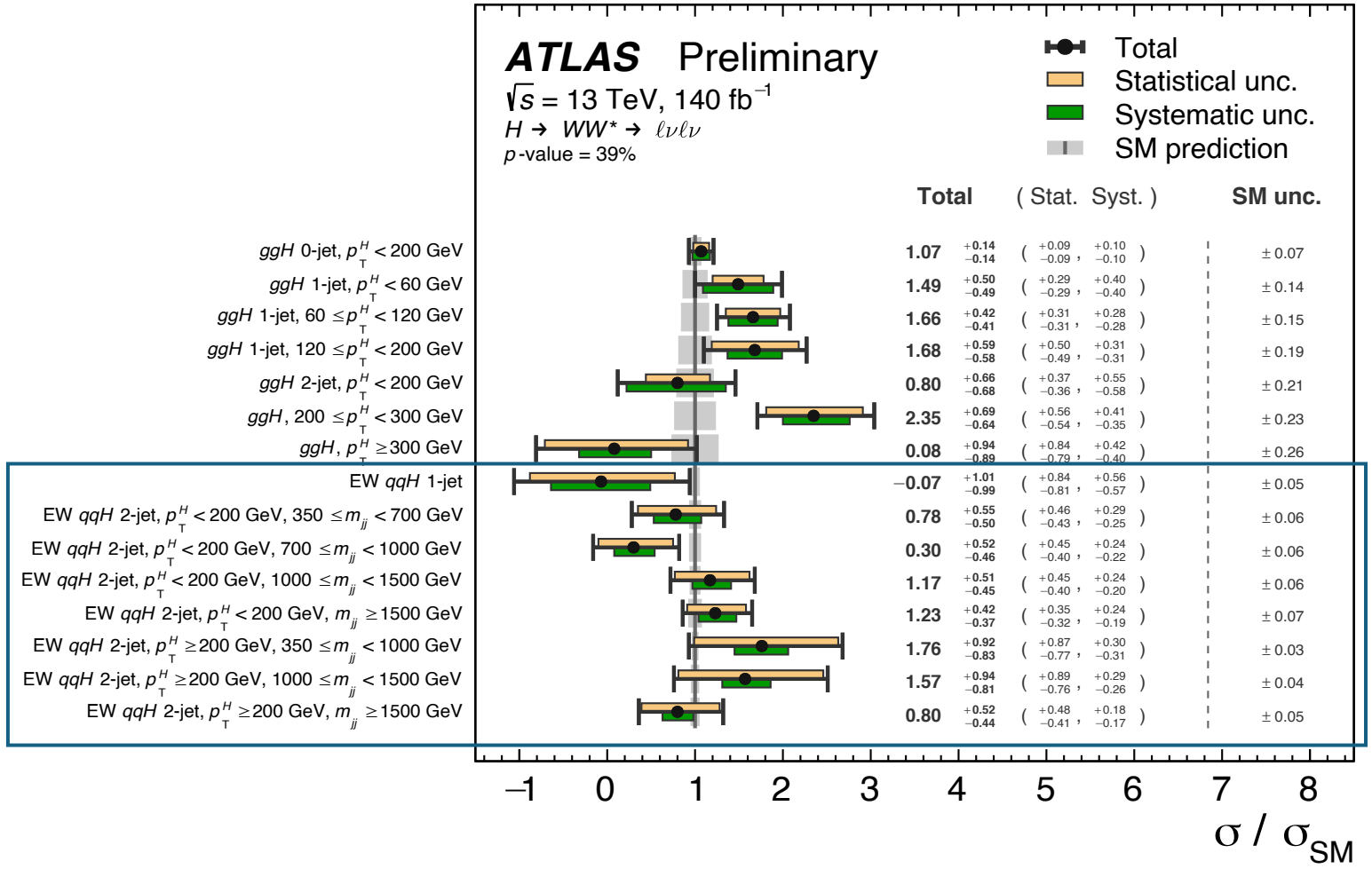

ggF and VBF $H \rightarrow WW^*$

CERN-EP-2025-054

Results:

- Measure σ_{ggF} and σ_{VBF}, and STXS cross-sections
- Compared to first 13 TeV paper:
  - 11% more precise for σ_{ggF} and σ_{VBF}.
  - 15 STXS categories resolved (11 last time)
  - 10-20% more precise for VBF STXS categories.
  - up to 35% improvement for ggF STXS categories.

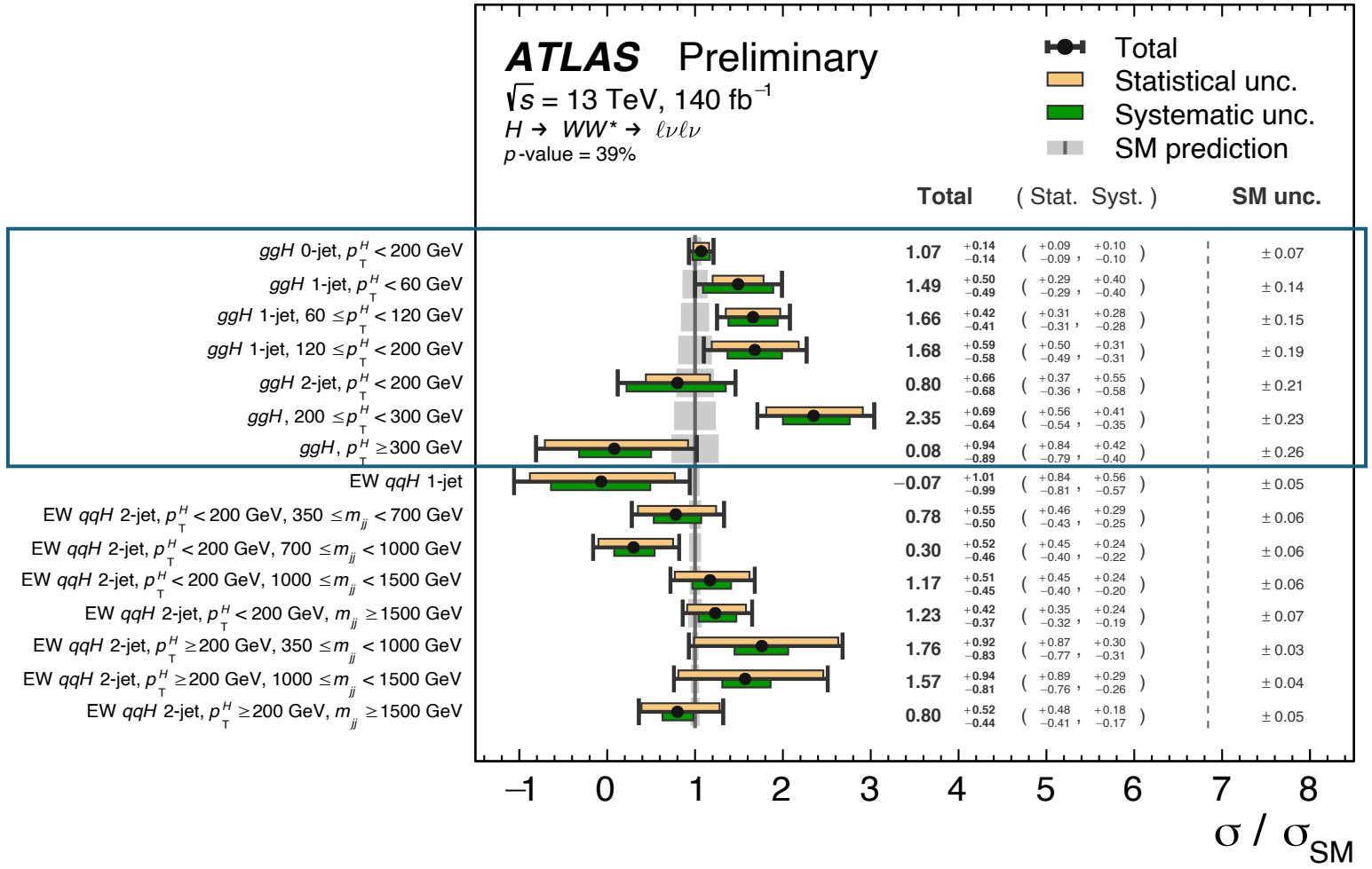

ggF and VBF $H \to WW^*$: EFT Interpretation

CERN-EP-2025-054

Strategy:

- Re-parameterize measured STXS signal strengths → constrain dim-6 CP-even EFT operators.
- PCA to find linear combinations of operators to which analysis has sensitivity.

Most contributing operators:

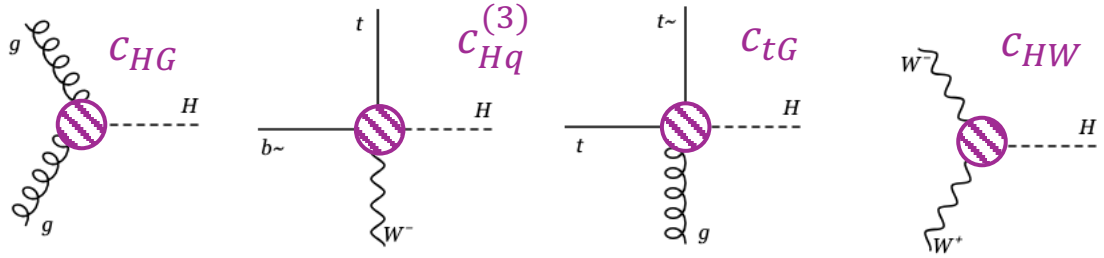

Results:

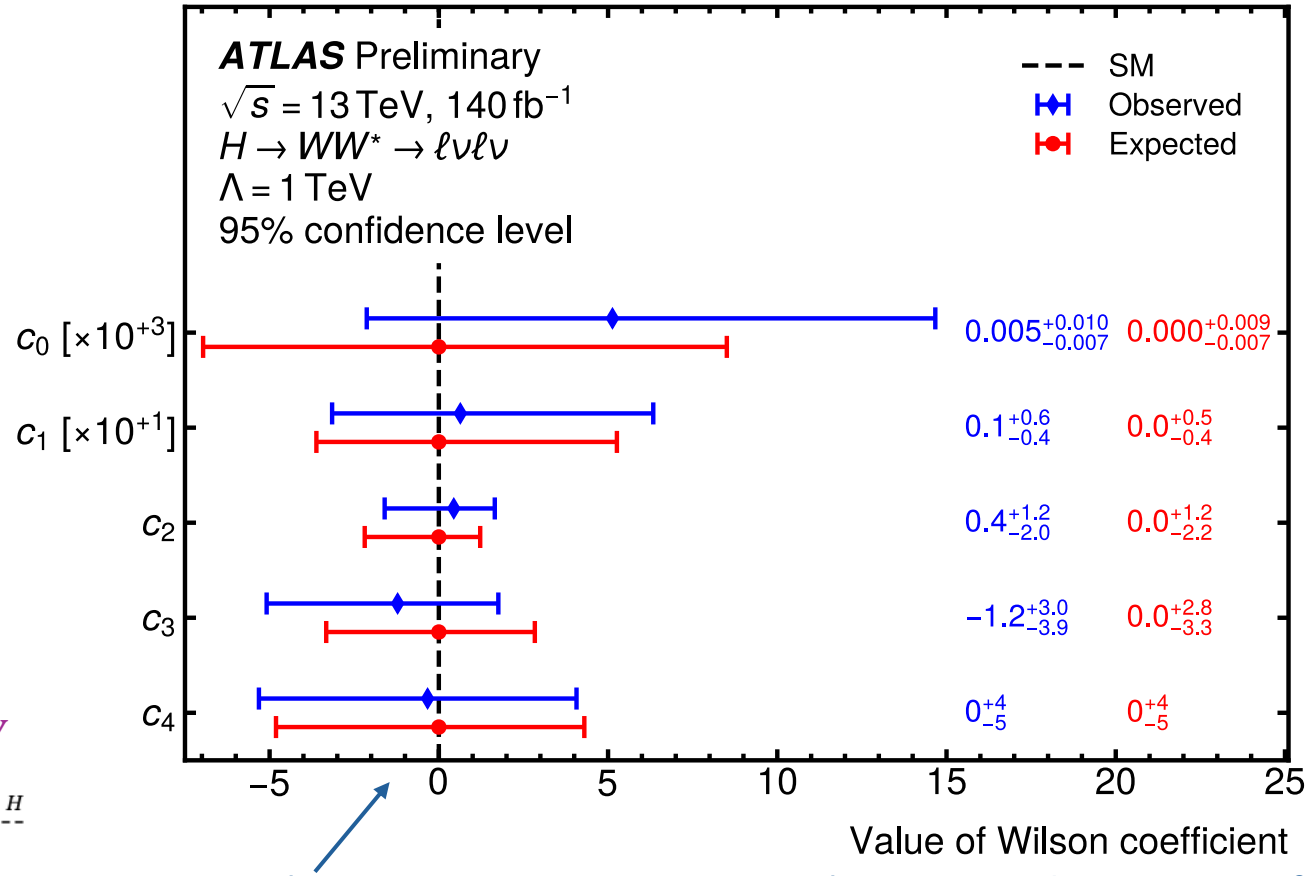

Simultaneous constraints on 5 linear combinations of EFT operators.

ggF and VBF $H \rightarrow WW^*$: CP-Sensitive EFT Interpretation

Strategy:

- Current STXS bins defined in CP-even variables → no sensitivity to CP violation.
- Analysis uses a CP-odd variable for CP sensitivity: azimuthal angle difference between the forward (highest η) and backward (lowest η) jets, $\Delta\phi_{jj}^{\pm}$.

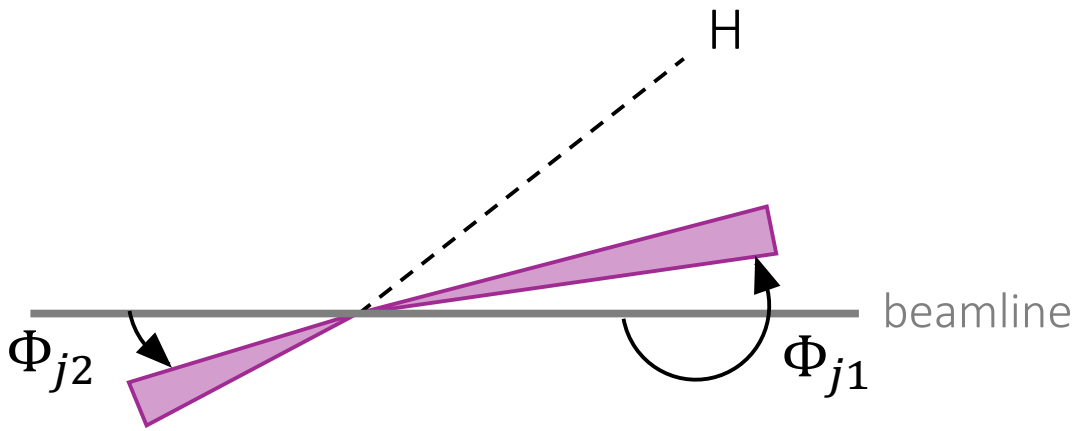

✓ This is **asymmetric around 0** for CP-odd/SM interference.

SM symmetric
Pure CP-odd terms symmetric w/phase shift
Mixed SM-CP-odd terms asymmetric

hep-ph/0703202

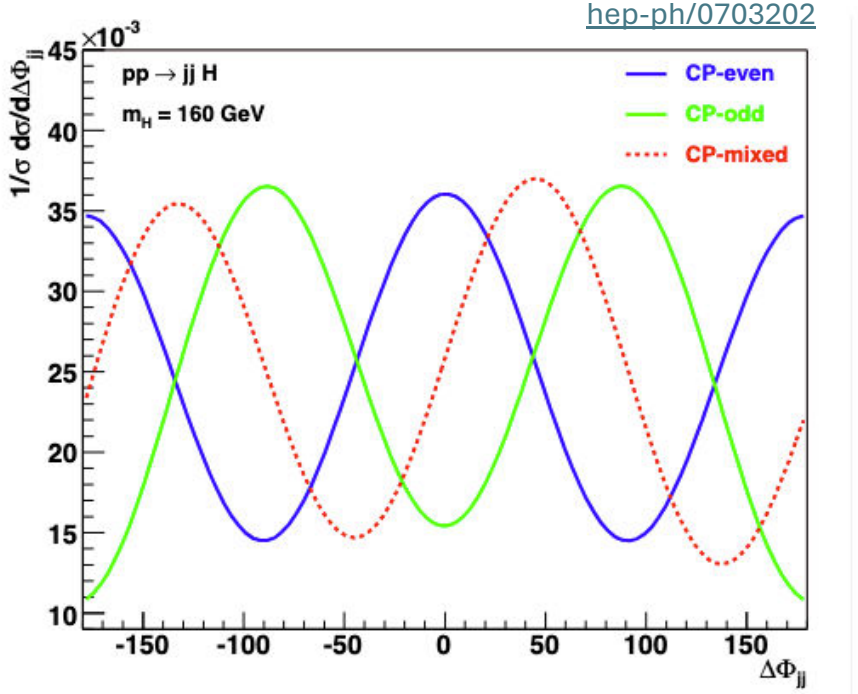

ggF and VBF $H \rightarrow WW^*$: CP-Sensitive EFT Interpretation

Strategy:

- Perform $STXS_{CP}$ measurement:
  - 2-jet STXS categories split into four $\Delta\phi_{jj}^{\pm}$ bins → target $c_{H\tilde{W}}, c_{H\tilde{G}}$
  - 0- and 1-jet STXS categories split as usual → target c_{HG}, c_{HW}.

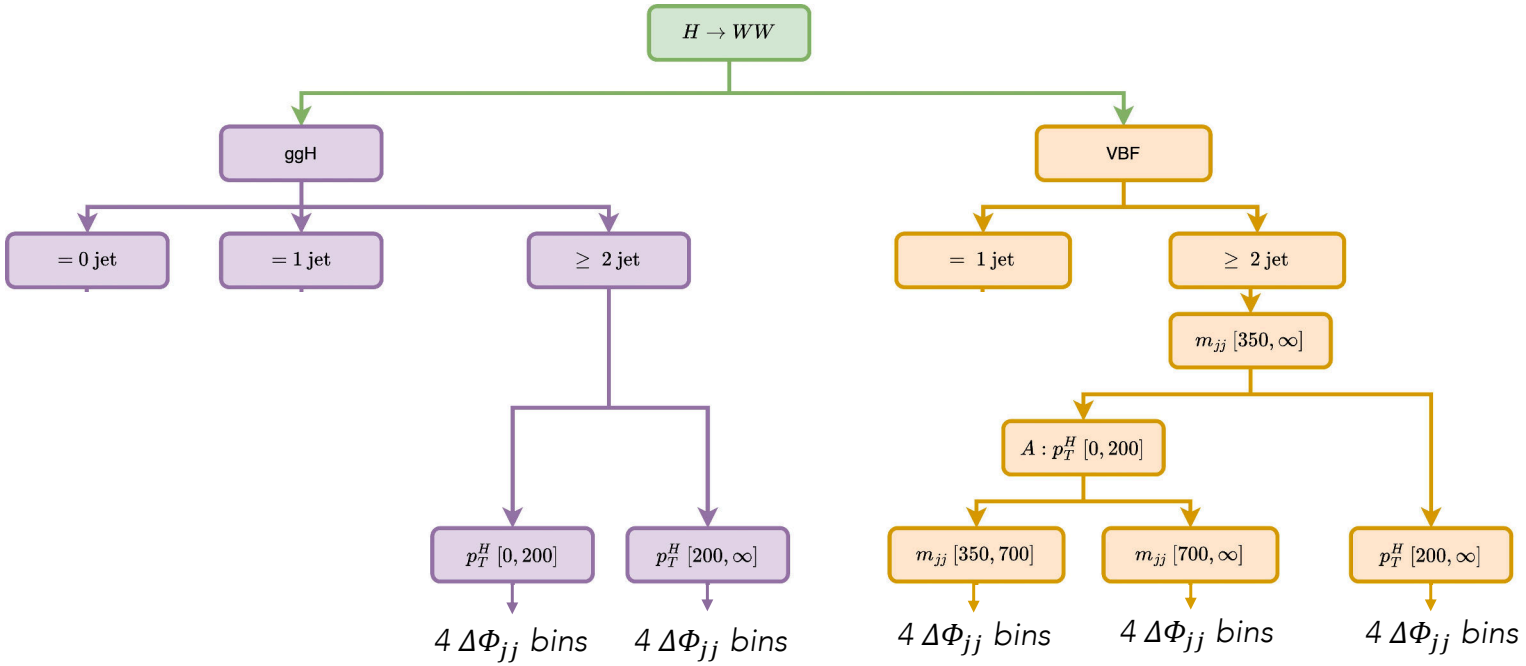

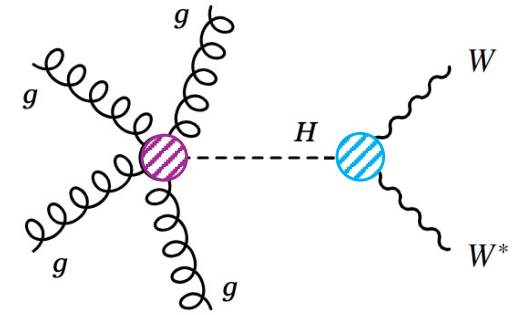

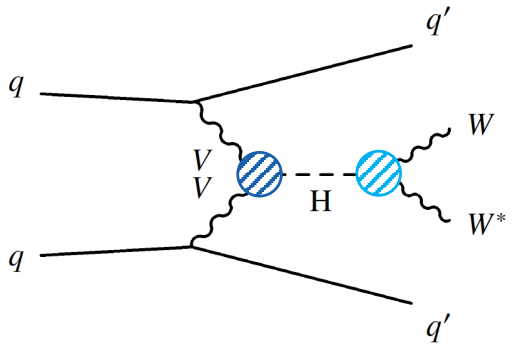

Affect Higgs production via ggF: $c_{HG}, c_{H\tilde{G}}$

Affect Higgs production via VBF: $c_{H\tilde{W}}$

Affect Higgs production via VBF and decay via *WW*: c_{HW}

ggF and VBF $H \to WW^*$: CP-Sensitive EFT Interpretation

Results:

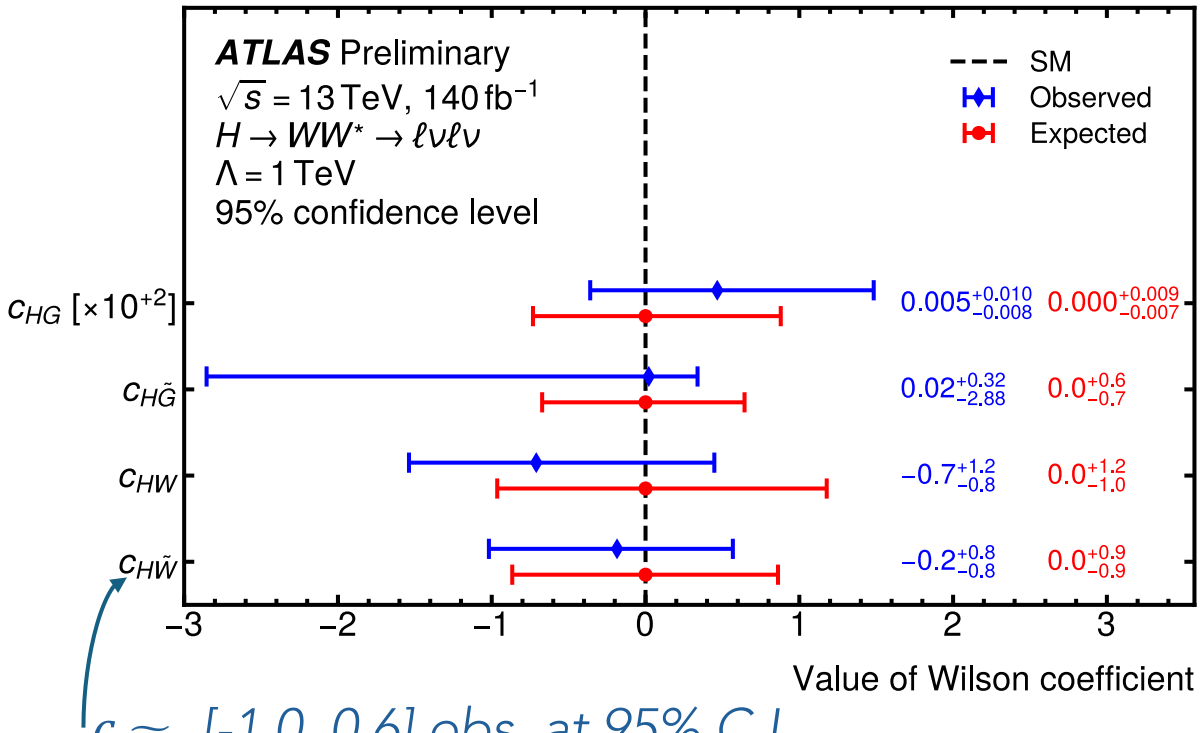

$c_{\widetilde{HW}}$ [-1.0, 0.6] obs. at 95% C.L.

- *Compare to world-leading limits from ATLAS Legacy Run 2 $H \to \tau\tau$ [HIGG-2022-07]: [−0.31, +0.88] obs at 95% C.L*
- *Advantages of this result: multi-POI fit, ~no correlation with CP-even effects, $\Delta\phi_{jj}^{\pm}$ is decay-agnostic.*

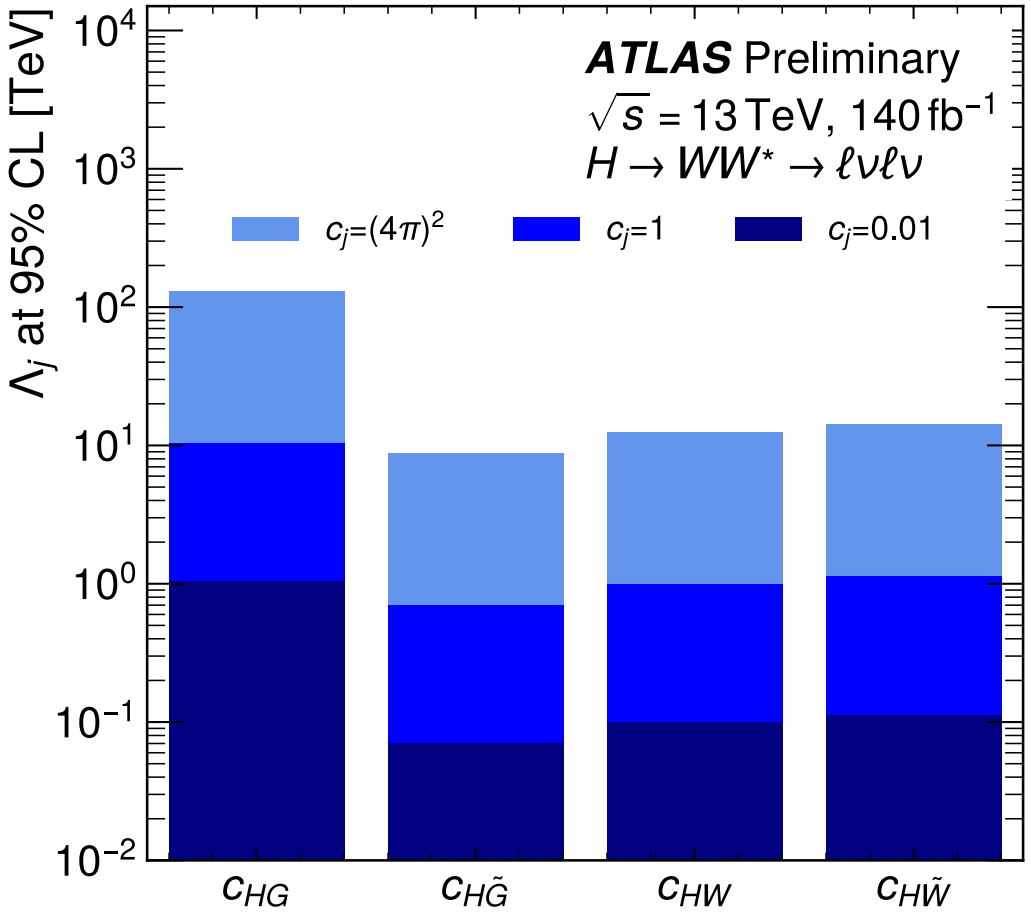

Limits on Wilson coefficients translated into limits on the energy scale of new physics.

VH $H \to WW^*$

HIGG-2023-09

Strategy:

- Target inclusive measurement (previously published) and VH STXS Stage 1.2 bins (new!)
- Channels for leptonic and hadronic V decays: same-sign (SS) 2ℓ, opposite-sign (OS) 2ℓ, 3ℓ and 4ℓ final states.
- Multivariate discriminants used in every channel.

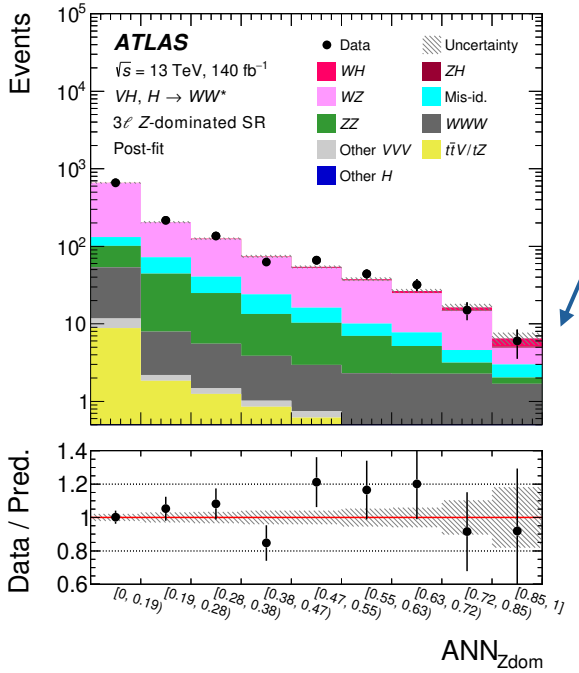

ANNs with nodes for signal and main bkgs for 2ℓ (OS) and 3ℓ

RNN for 2ℓ (SS) due to varying jet multiplicities

BDT for 4ℓ (mainly ZZ bkg)

eg. 3ℓ channel:

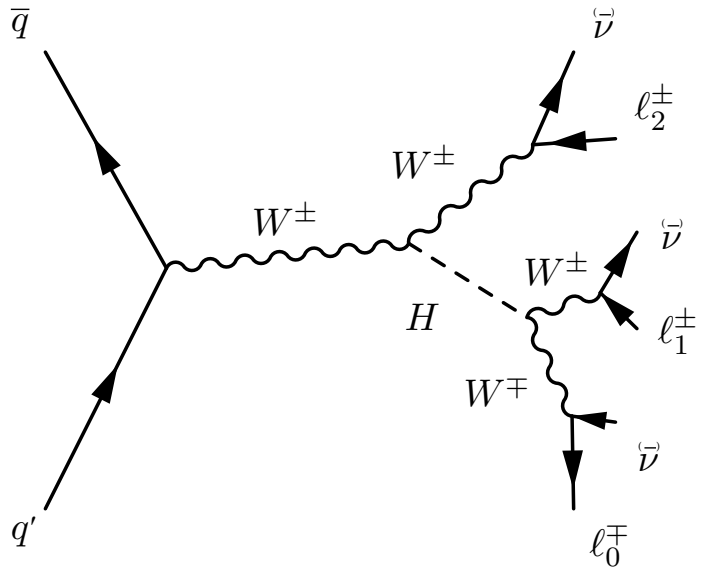

VH $H \to WW^*$

HIGG-2023-09

Results (Inclusive):

- Measurements of WH and ZH cross-sections compatible with SM within 95% C.L:

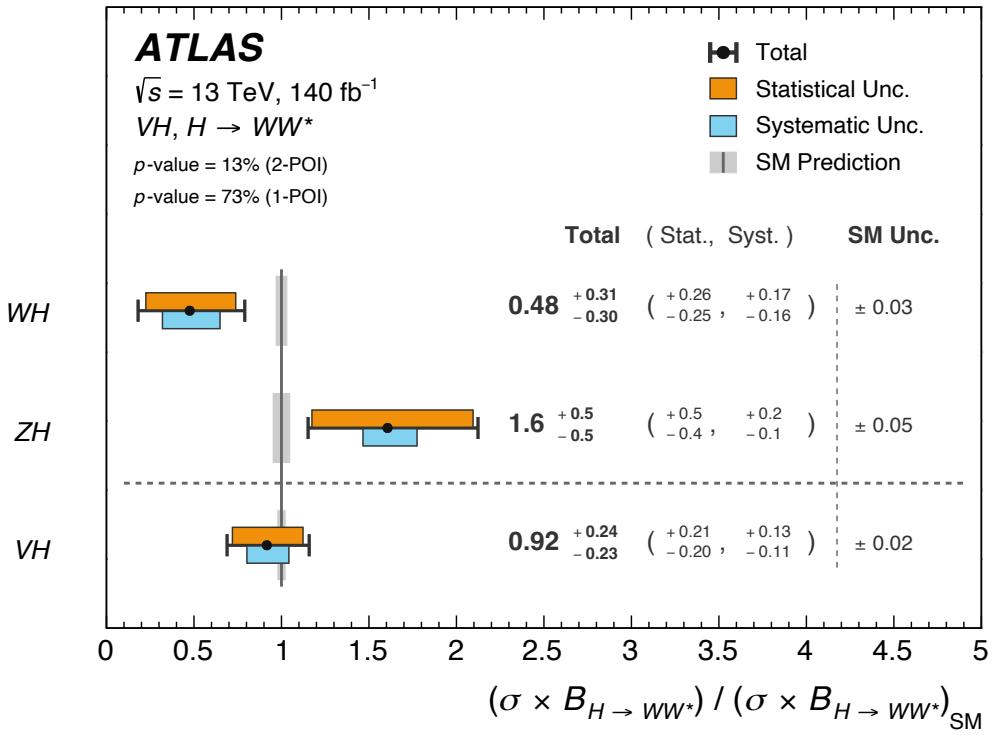

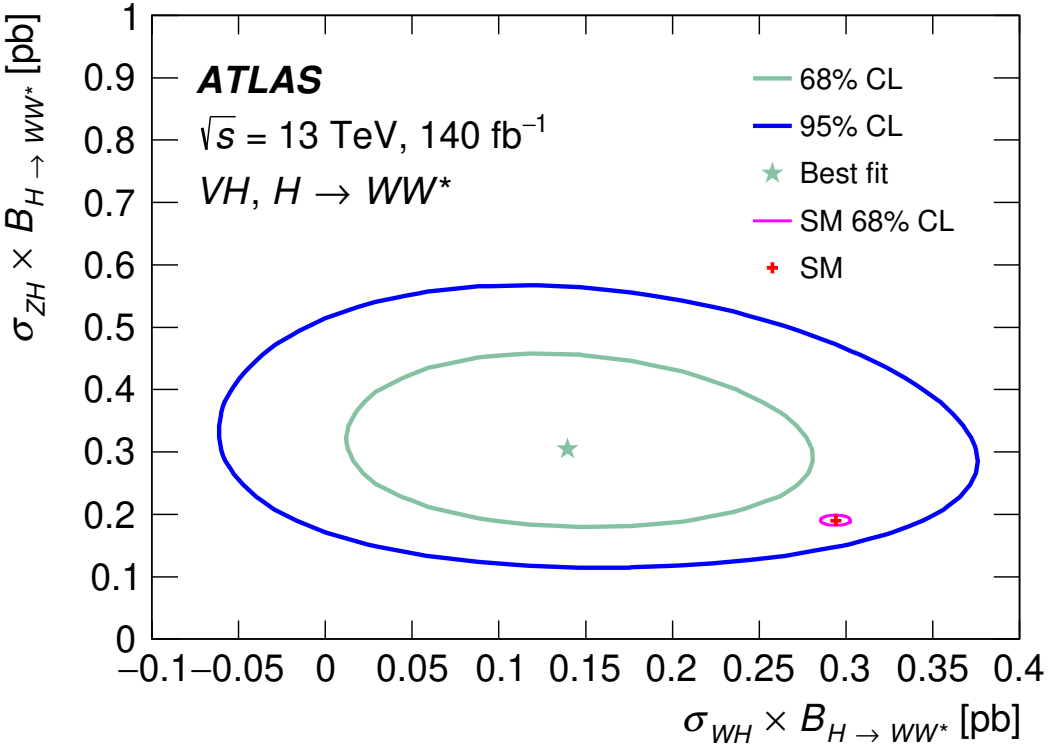

- Dominant uncertainties are statistical; 3ℓ and 4ℓ channels dominate sensitivity.

VH $H \to WW^*$

HIGG-2023-09

Strategy (STXS):

- Signal regions split by p_{T}^{V} proxy for STXS measurement:
  - 2ℓ, 4ℓ: sums of lepton & jet p_{T} and missing energy
  - 3ℓ: Regression ANN

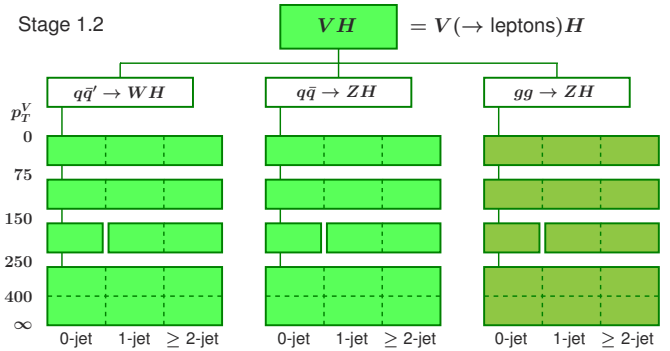

Results (STXS):

WH, ZH and EW qqH split according to STXS 1.2 scheme

Lower cut-off: LH becomes unphysical (negative S+B)

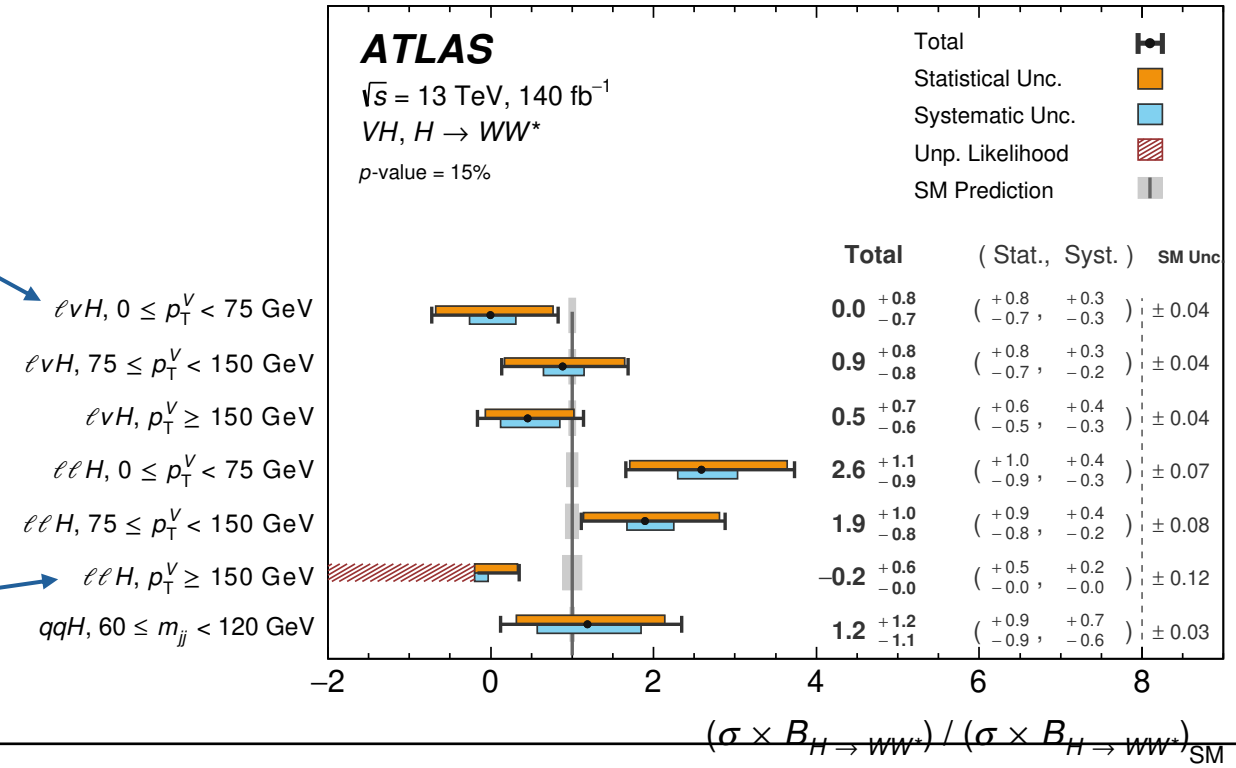

Excellent $p_{\mathrm{T}}^{V} < 150$ GeV sensitivity (competitive with combination!)

Combination of Run 2 STXS Measurements

Combinations of Run 2 Higgs boson measurements performed by ATLAS and CMS at the end of Run 2, published in Nature.

New for Moriond: **CMS combination** of Run 2 STXS measurements.

- ✓ First CMS STXS combination
- ✓ Updated input measurements wrt Nature paper.

Combination of Run 2 STXS Measurements

CMS-PAS-HIG-21-018
(link not public yet)

See Aliya Nigamova's wildcard talk for more!

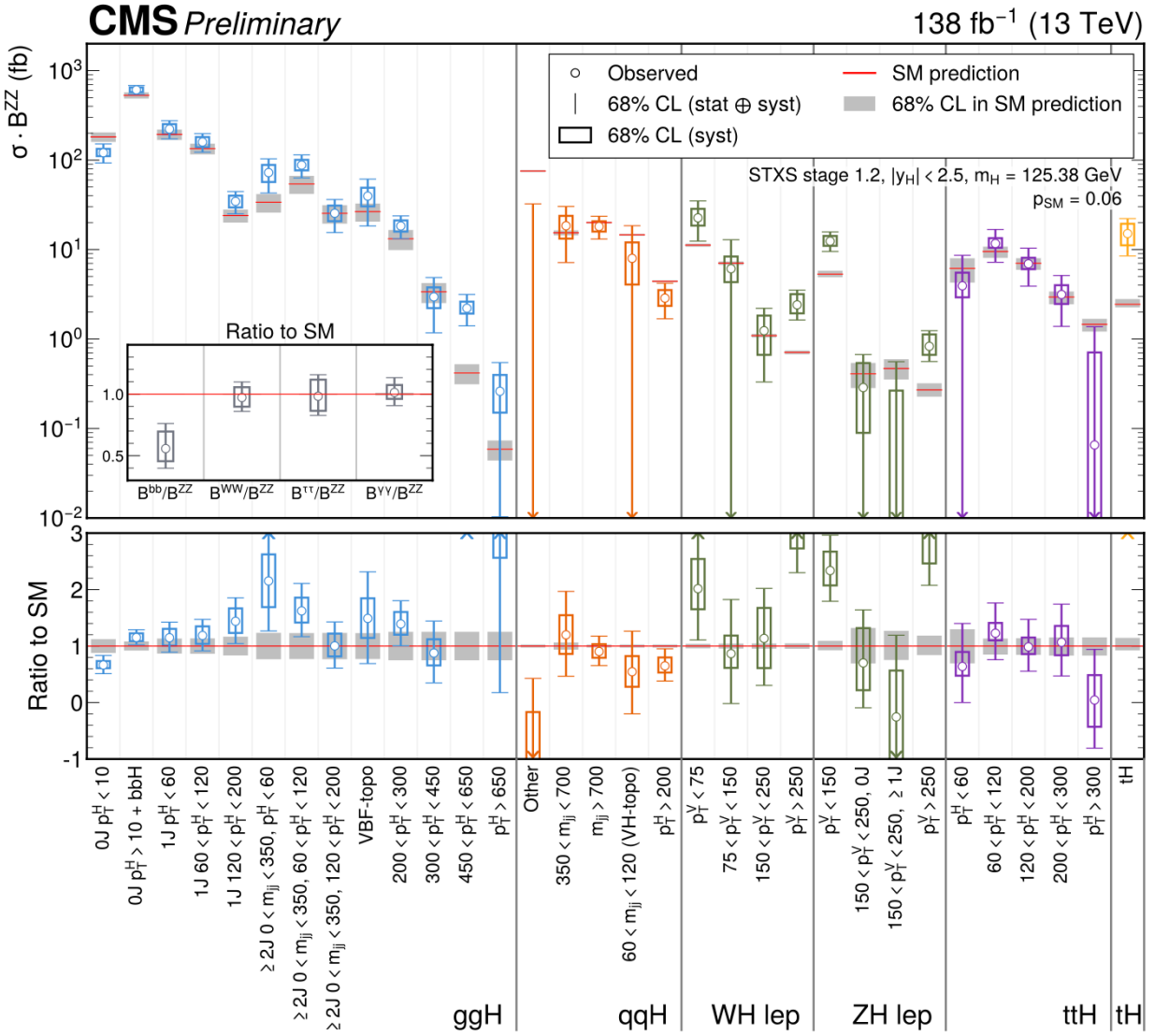

Conclusion

- Presented several measurements of total and differential Higgs boson production that are **new for Moriond**.
- In many cases, huge improvement over existing Run 2 results, with same dataset → innovative analysis techniques and improvement in combined performance.
- Run 3 and beyond bring more promise for discovery.

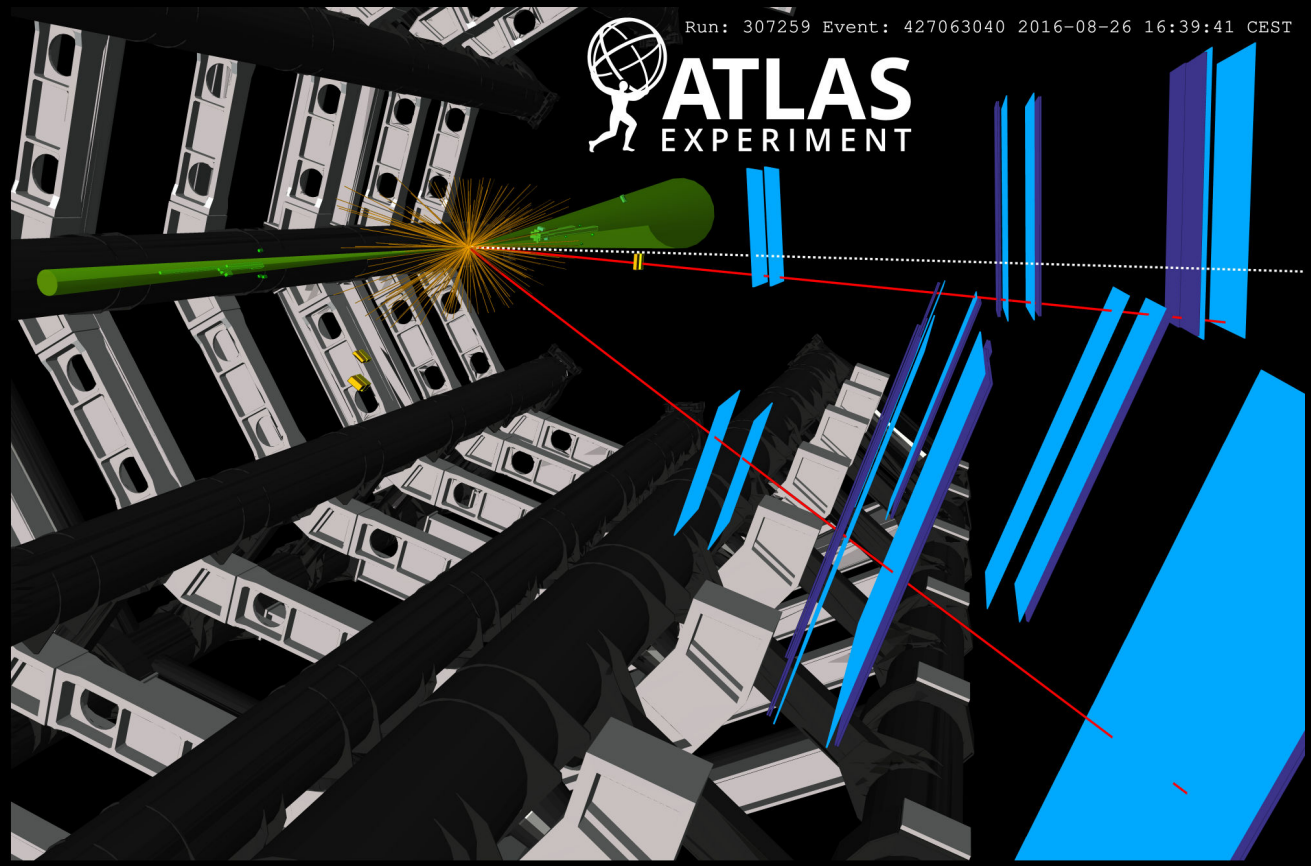

Backup

ggF and VBF $H \to WW^*$

Strategy:

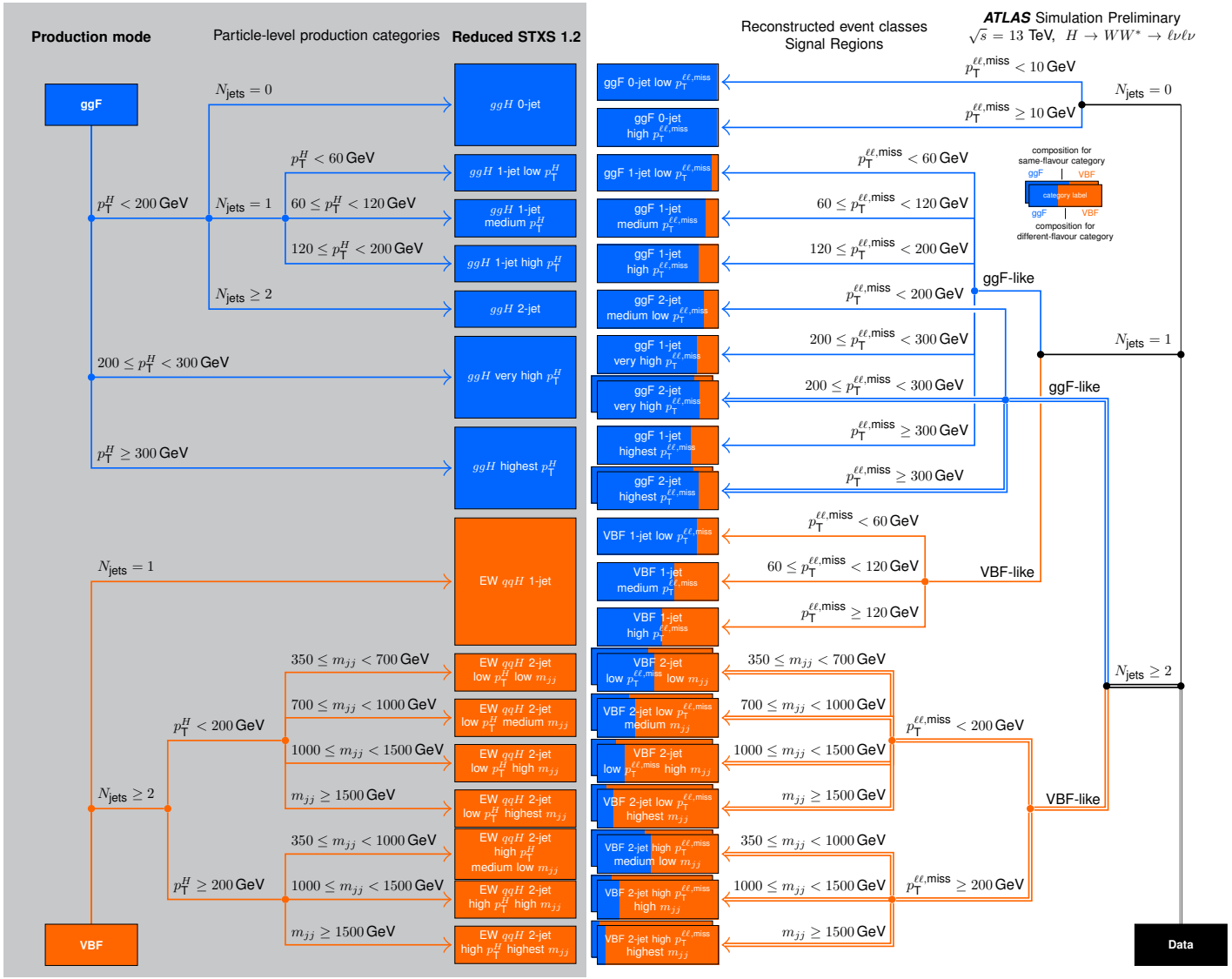

ggF and VBF $H \rightarrow WW^*$

Strategy:

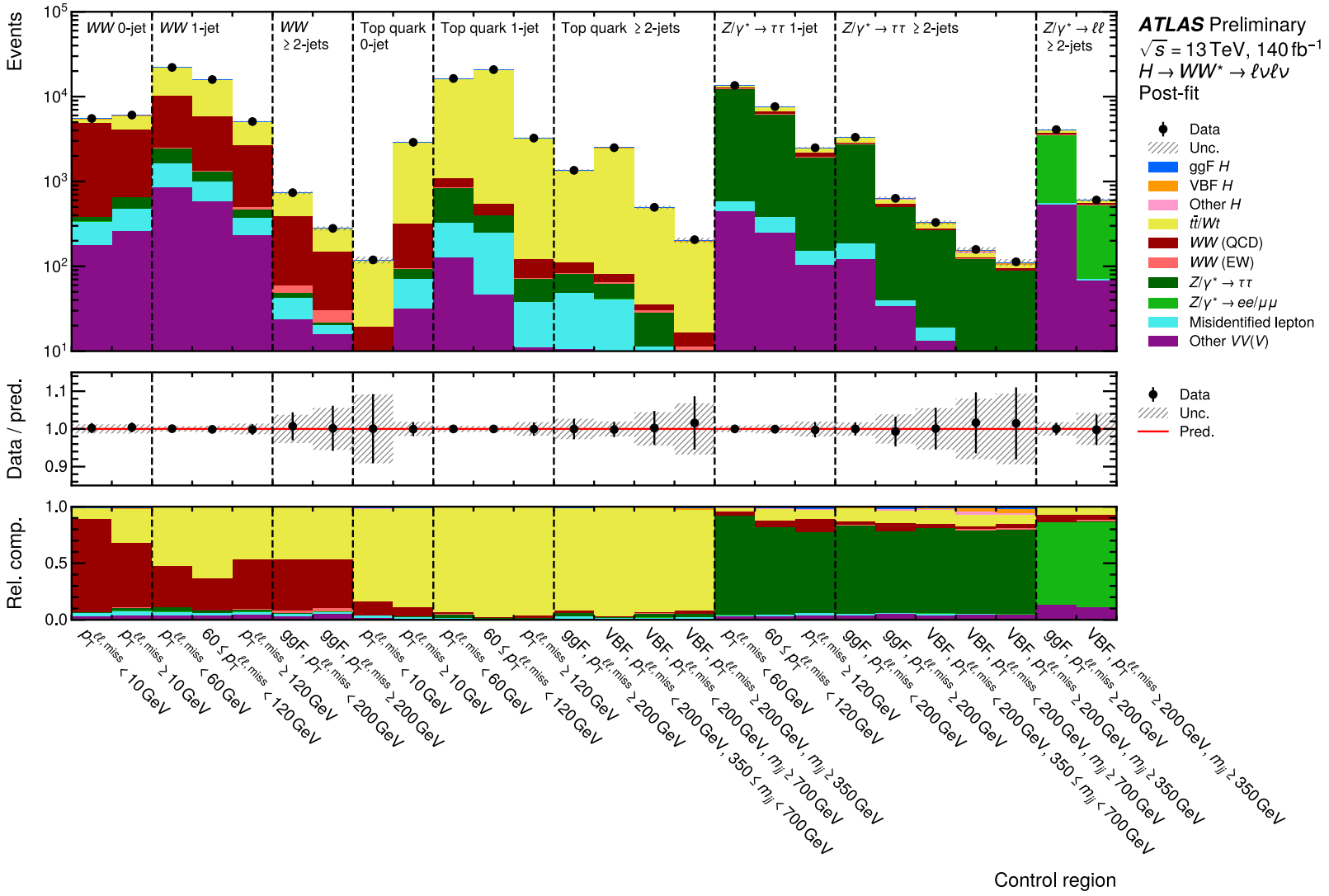

ggF and VBF $H \rightarrow WW^*$

Strategy:

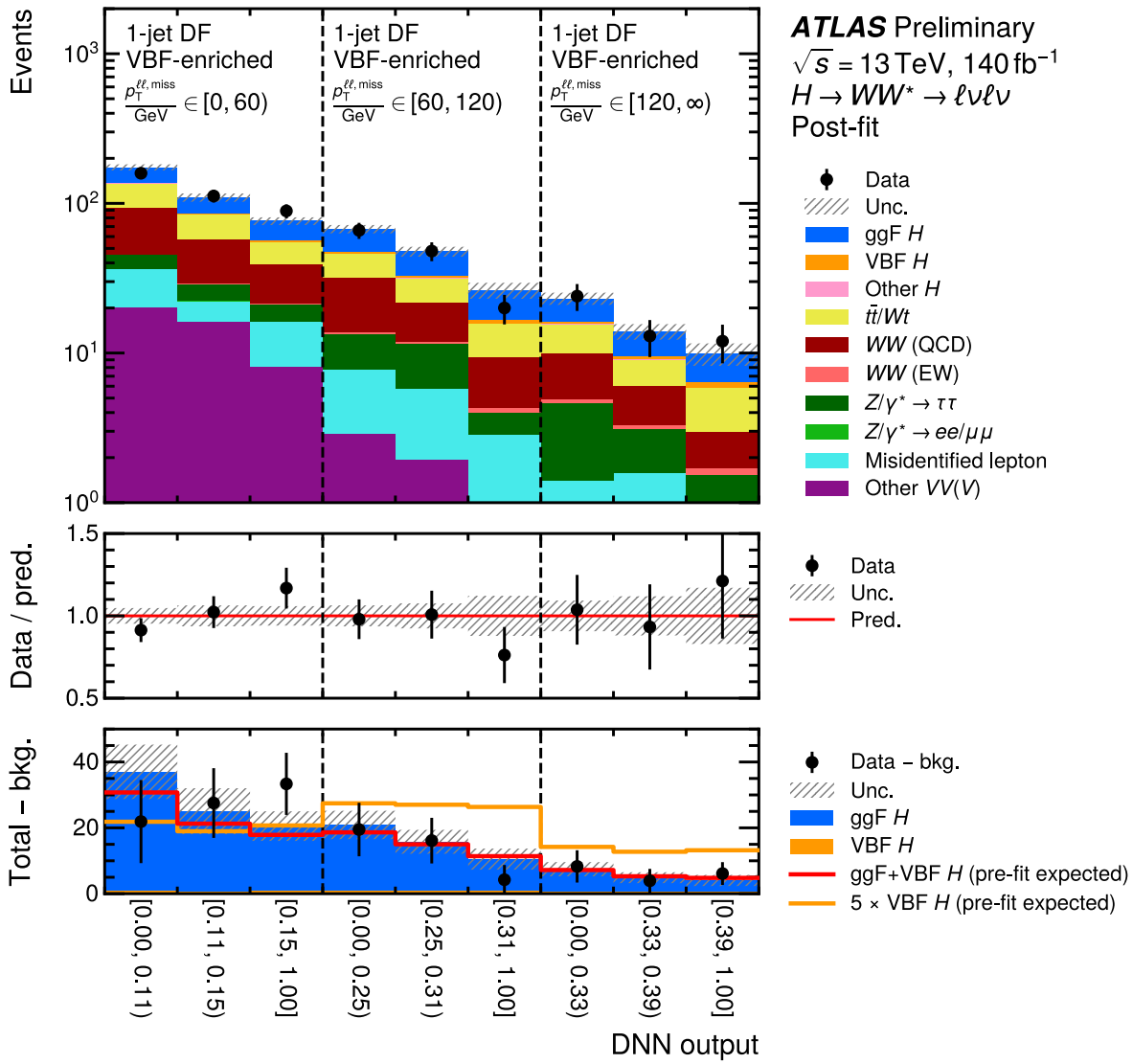

ggF and VBF $H \rightarrow WW^*$

Results:

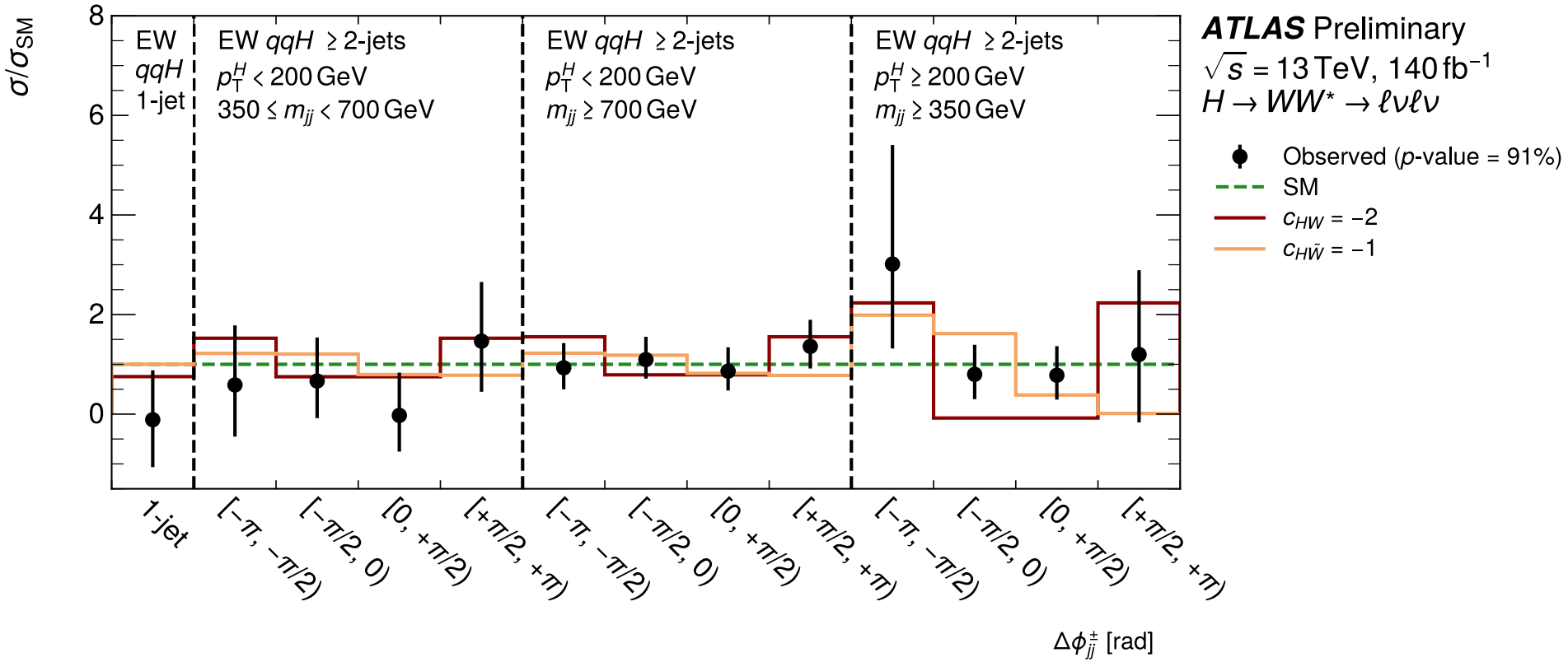

ggF and VBF $H \rightarrow WW^*$

Results:

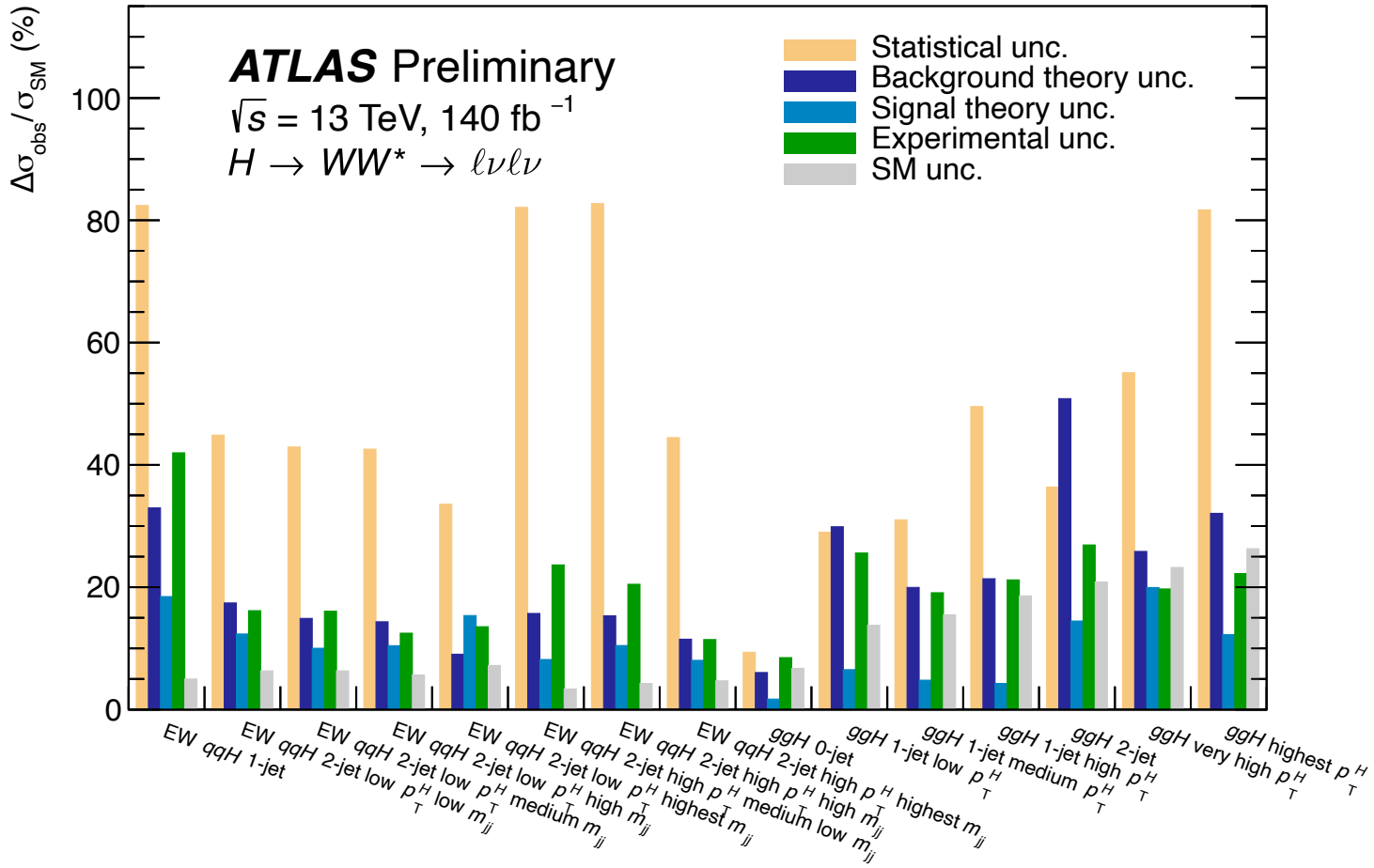

VH $H \to WW^*$

Strategy:

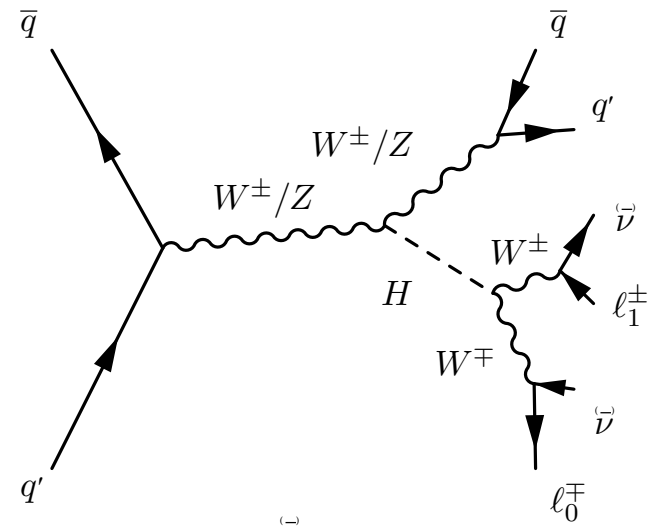

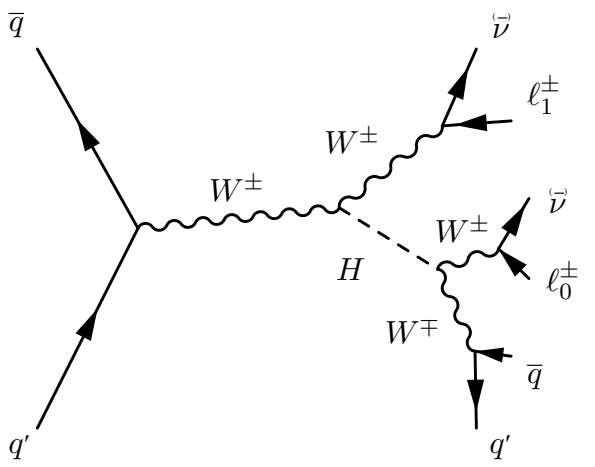

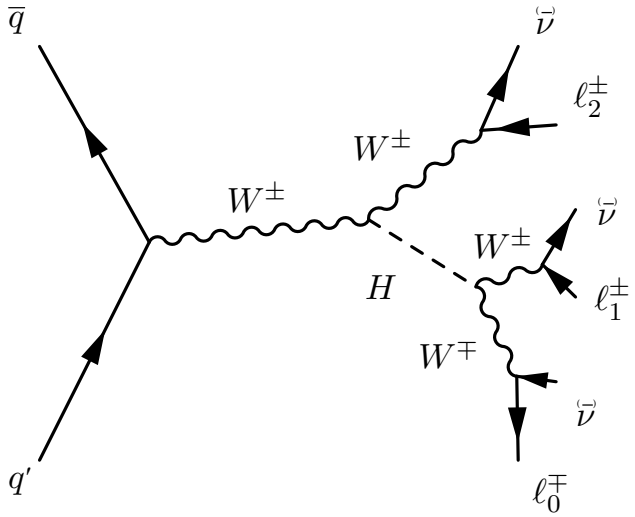

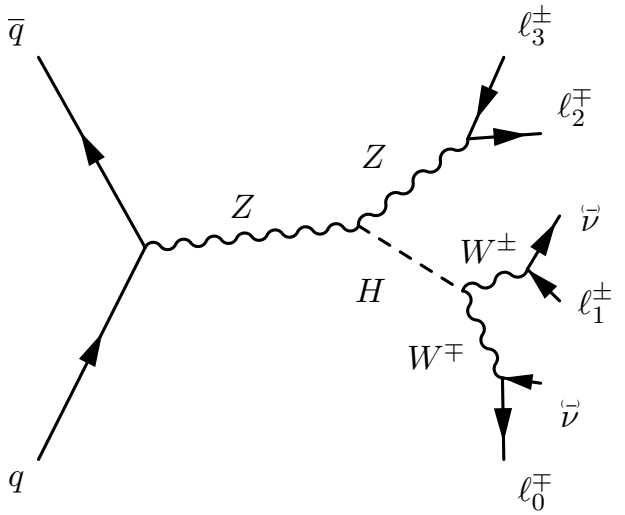

VH $H \to WW^*$

Strategy:

Channel	p_{T}^{V} proxy	Reconstructed SR	Relevant p_{T}^{V} range
Opposite-sign 2ℓ	Dijet transverse momentum, p_{T}^{jj}	$0 < p_{\mathrm{T}}^{jj} < 160$ GeV $160 < p_{\mathrm{T}}^{jj} < 260$ GeV $p_{\mathrm{T}}^{jj} > 260$ GeV	$0 < p_{\mathrm{T}}^{V} < 150$ GeV $150 < p_{\mathrm{T}}^{V} < 250$ GeV $p_{\mathrm{T}}^{V} > 250$ GeV
Same-sign 2ℓ	Scalar sum of lepton, jet, and missing transverse momenta, $\sum \lvert p_{\mathrm{T}} \rvert$	$0 < \sum \lvert p_{\mathrm{T}} \rvert < 200$ GeV $200 < \sum \lvert p_{\mathrm{T}} \rvert < 320$ GeV $320 < \sum \lvert p_{\mathrm{T}} \rvert < 460$ GeV $\sum \lvert p_{\mathrm{T}} \rvert > 460$ GeV	$0 < p_{\mathrm{T}}^{V} < 75$ GeV $75 < p_{\mathrm{T}}^{V} < 150$ GeV $150 < p_{\mathrm{T}}^{V} < 250$ GeV $p_{\mathrm{T}}^{V} > 250$ GeV
3ℓ Z-dominated	Regression ANN for W transverse momentum, p_{T}^{R}	$0 < p_{\mathrm{T}}^{R} < 90$ GeV $90 < p_{\mathrm{T}}^{R} < 180$ GeV $p_{\mathrm{T}}^{R} > 180$ GeV	$0 < p_{\mathrm{T}}^{V} < 75$ GeV $75 < p_{\mathrm{T}}^{V} < 150$ GeV $p_{\mathrm{T}}^{V} > 150$ GeV
3ℓ Z-depleted	Regression ANN for W transverse momentum, p_{T}^{R}	$0 < p_{\mathrm{T}}^{R} < 90$ GeV $90 < p_{\mathrm{T}}^{R} < 180$ GeV $180 < p_{\mathrm{T}}^{R} < 270$ GeV $p_{\mathrm{T}}^{R} > 270$ GeV	$0 < p_{\mathrm{T}}^{V} < 75$ GeV $75 < p_{\mathrm{T}}^{V} < 150$ GeV $150 < p_{\mathrm{T}}^{V} < 250$ GeV $p_{\mathrm{T}}^{V} > 250$ GeV
4ℓ	Z boson transverse momentum, p_{T}^{Z}	$0 < p_{\mathrm{T}}^{Z} < 75$ GeV $75 < p_{\mathrm{T}}^{Z} < 150$ GeV $150 < p_{\mathrm{T}}^{Z} < 250$ GeV $p_{\mathrm{T}}^{Z} > 250$ GeV	$0 < p_{\mathrm{T}}^{V} < 75$ GeV $75 < p_{\mathrm{T}}^{V} < 150$ GeV $150 < p_{\mathrm{T}}^{V} < 250$ GeV $p_{\mathrm{T}}^{V} > 250$ GeV

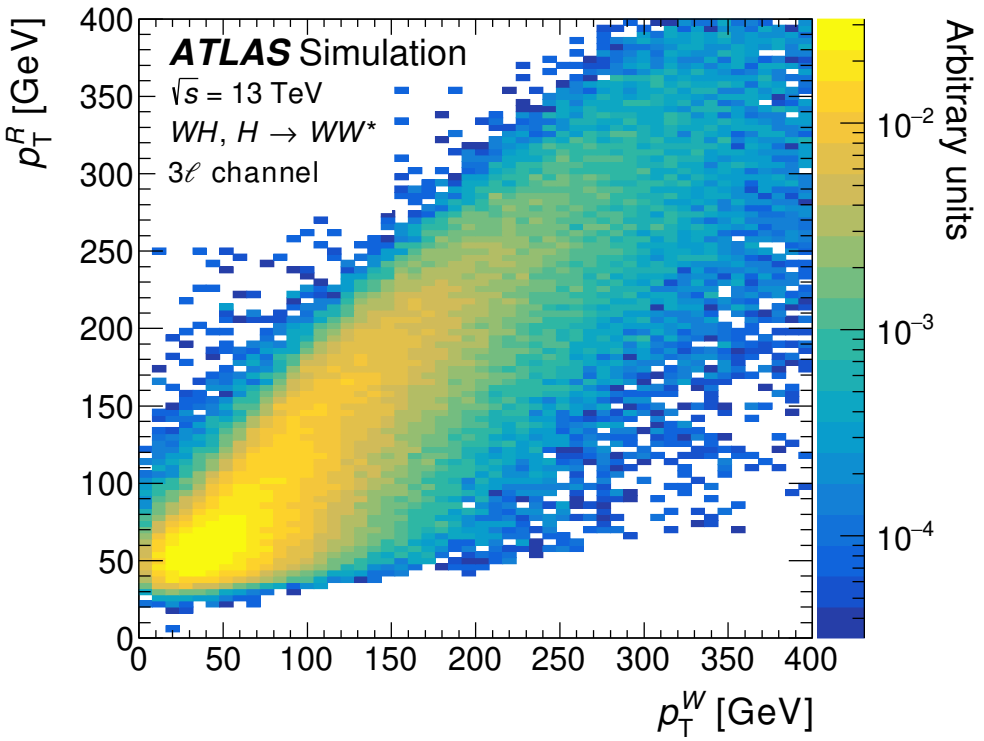

VH $H \rightarrow WW^*$

Results:

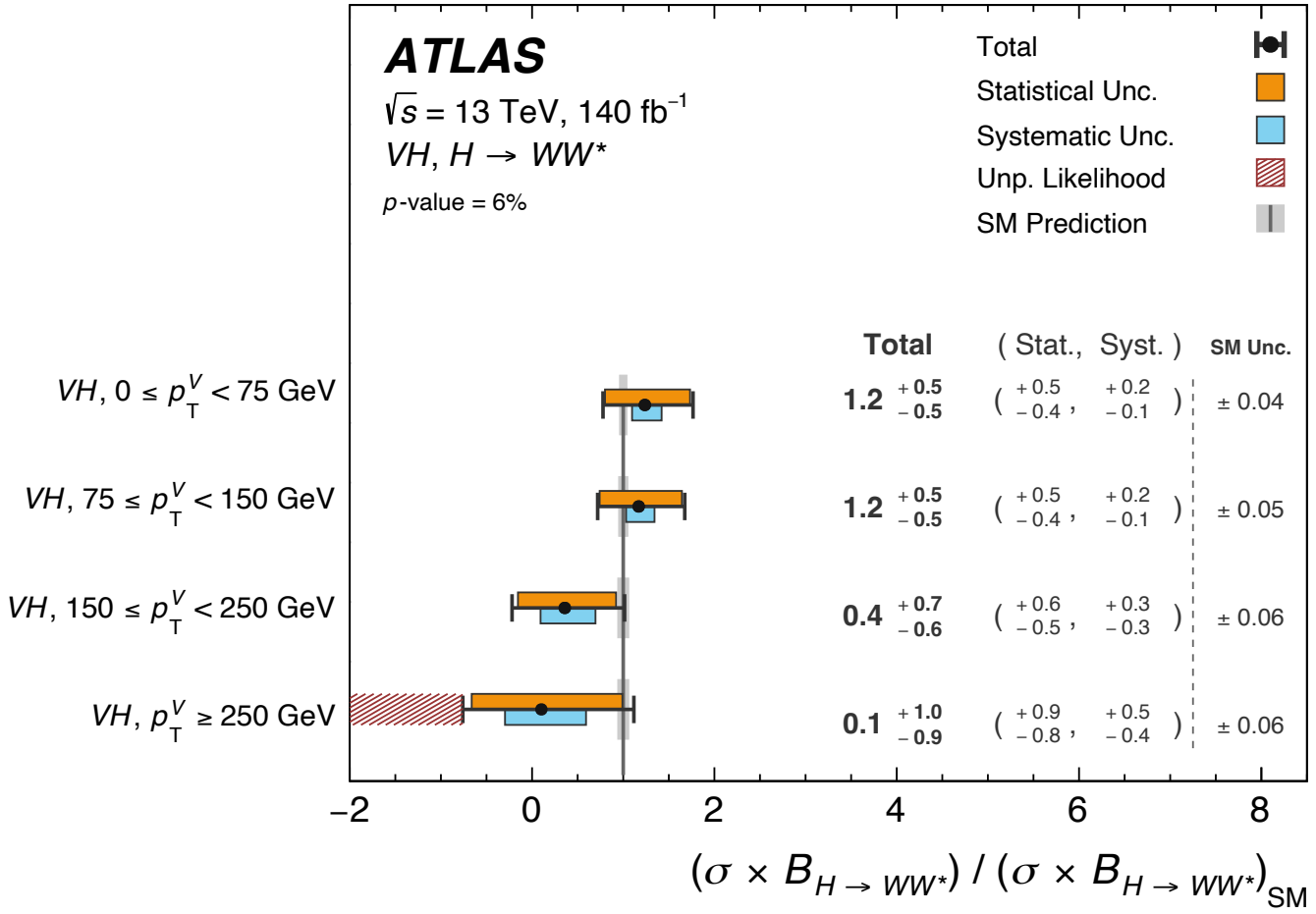

Recent Run 3 Results

Recent Run 3 Results

Several Higgs measurements among the earliest LHC Run 3 results.

- New COM energy: 13.6 TeV
- Use 2022 data: 20-35 fb^{-1}

ref

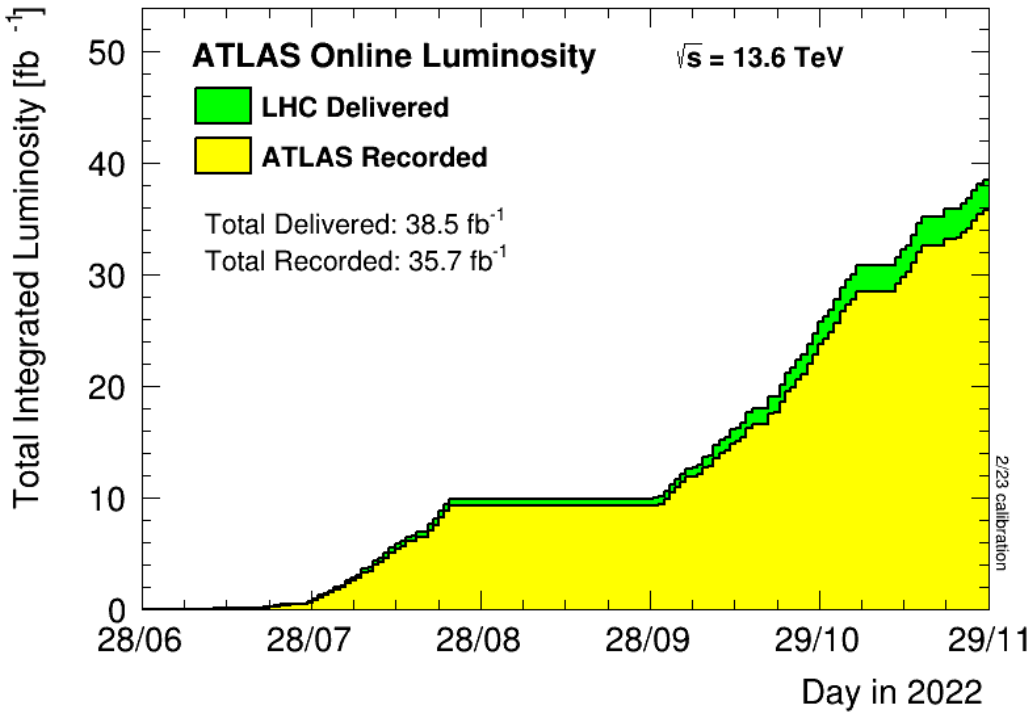

ref

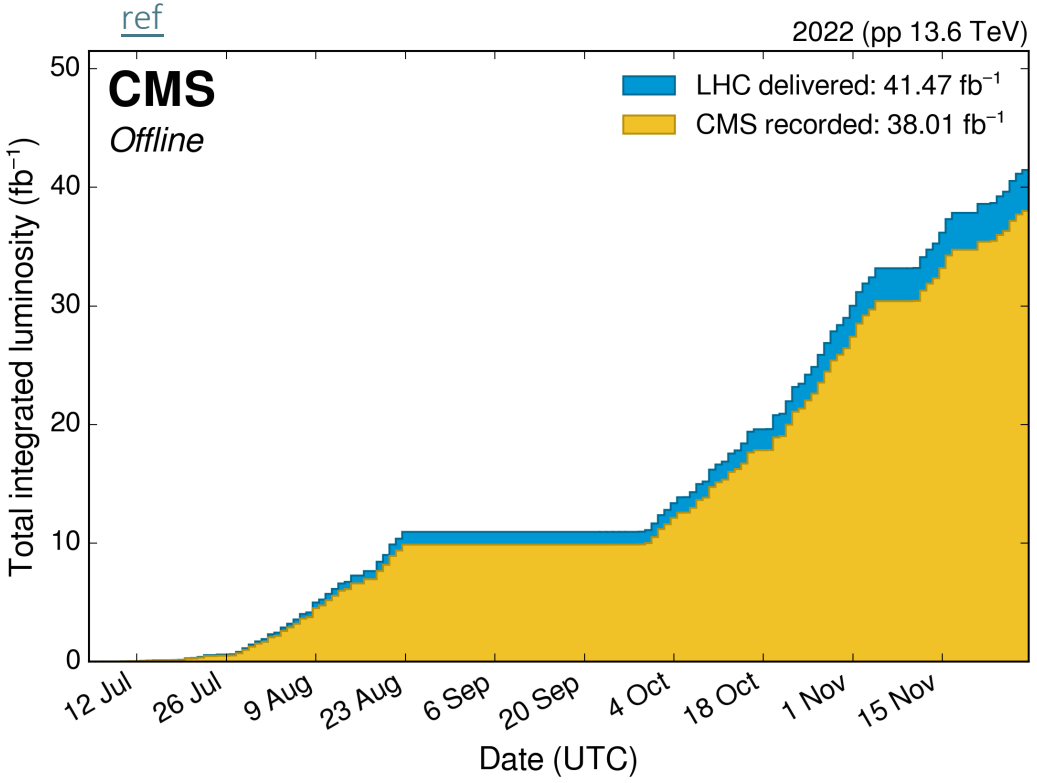

Recent Run 3 Results

Take advantage of cleanest Higgs boson decay channels:

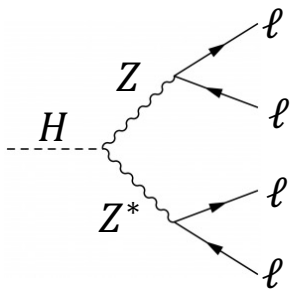

tracks and calo deposits from electrons and muons

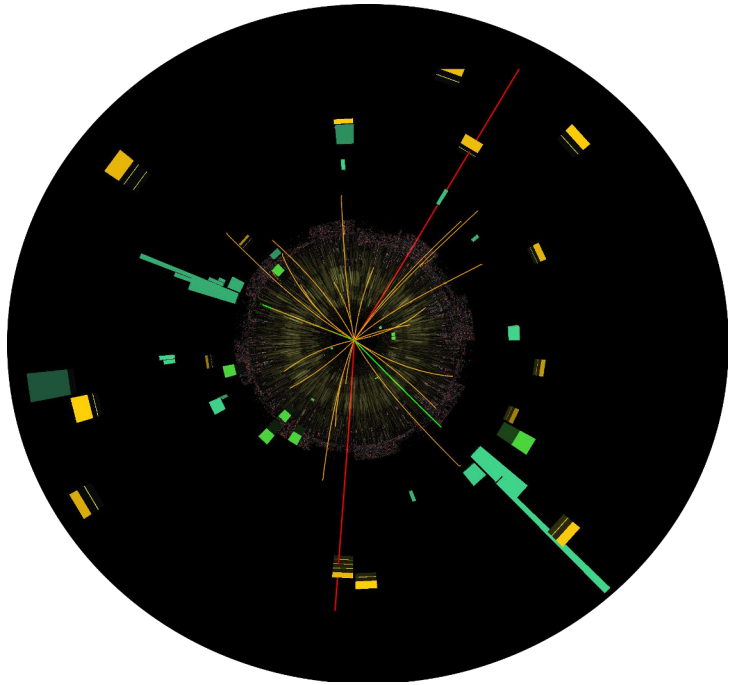

$H \to ZZ^* \to 4\ell$

calo deposits from photons

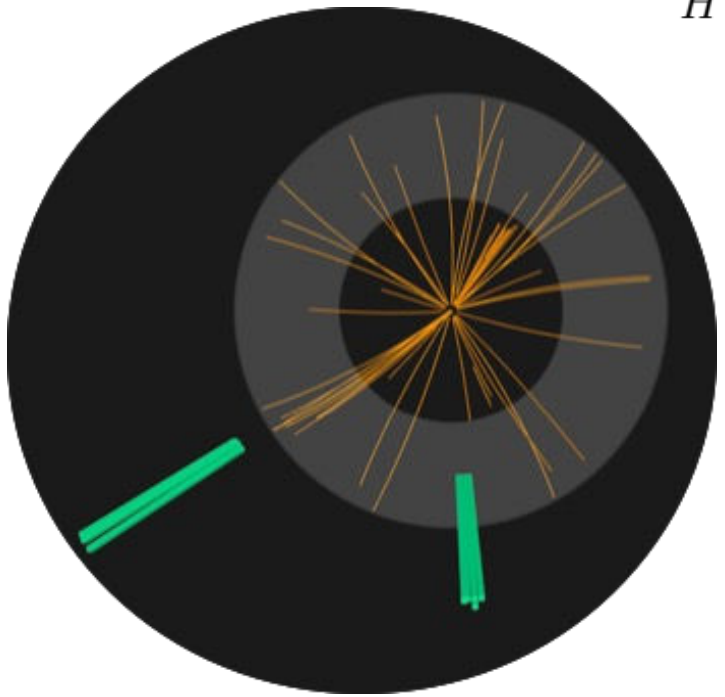

$H \to \gamma\gamma$

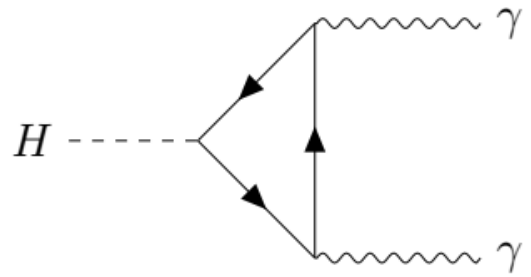

HIGG-2022-12

13.6 TeV Cross-Section Measurements

ATLAS 13.6 TeV $H \to ZZ^*$ and $H \to \gamma\gamma$ [HIGG-2022-12]

Aim:

- Measure 13.6 TeV cross-section of Higgs production (all modes included).

Strategy:

- Fiducial phase spaces defined for both analyses.

$H \to \gamma\gamma$

Photons	
Leading (sub-leading) p_{T}^{γ}	$p_{\mathrm{T}}^{\gamma}/m_{\gamma\gamma} > 0.35(0.25)$
Pseudorapidity	$\lvert\eta\rvert < 2.37$ and outside $1.37 < \lvert\eta\rvert < 1.52$
Isolation ($\Delta R = 0.2$)	$E_{\mathrm{T}}^{\mathrm{iso}}/E_{\mathrm{T}}^{\gamma} < 0.05$
Di-photon system	
Mass window	$105\,\mathrm{GeV} < m_{\gamma\gamma} < 160\ \mathrm{GeV}$

$H \to ZZ^*$

Leptons	
Leptons	$p_{\mathrm{T}} > 5$ GeV, $\lvert\eta\rvert < 2.7$
Lepton selection and pairing	
Lepton kinematics	$p_{\mathrm{T}} > 20, 15, 10$ GeV
Leading pair (m_{12})	SFOC lepton pair with smallest $\lvert m_Z - m_{\ell\ell}\rvert$
Subleading pair (m_{34})	remaining SFOC lepton pair with smallest $\lvert m_Z - m_{\ell\ell}\rvert$
Event selection (at most one quadruplet per event)	
Mass requirements	50 GeV$< m_{12} <$ 106 GeV and 12 GeV$< m_{34} <$ 115 GeV
Lepton separation	$\Delta R(\ell_i, \ell_j) > 0.1$
J/ψ veto	$m(\ell_i, \ell_j) > 5$ GeV for all SFOC lepton pairs
Mass window	105 GeV$< m_{4\ell} <$ 160 GeV
If extra lepton with $p_{\mathrm{T}} > 12$ GeV	quadruplet with largest matrix element value

13.6 TeV Cross-Section Measurements

ATLAS 13.6 TeV $H \to ZZ^*$ and $H \to \gamma\gamma$ [HIGG-2022-12]

Strategy:

- Signal extracted via fit to invariant mass spectra.

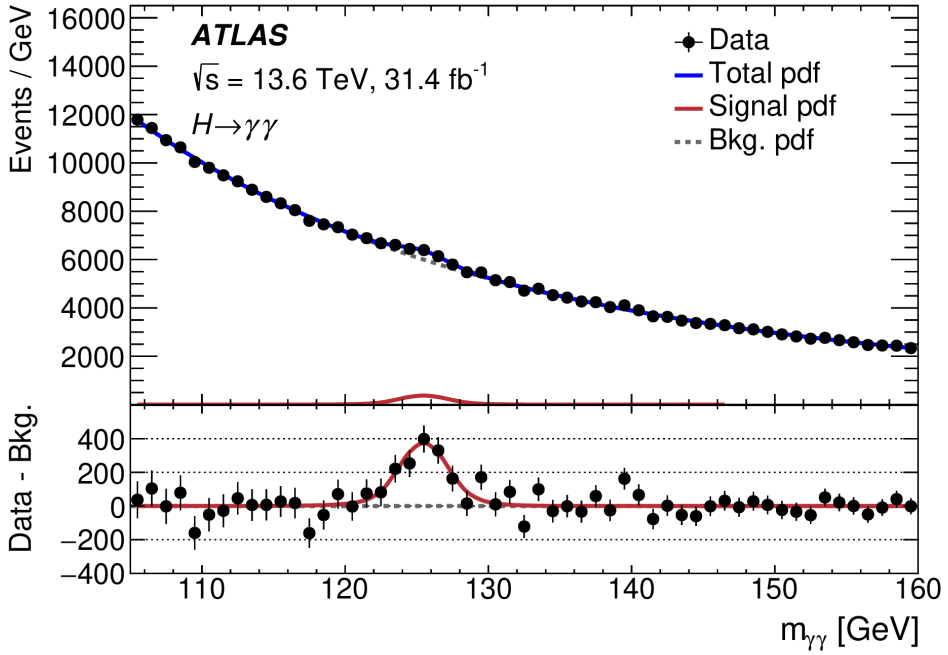

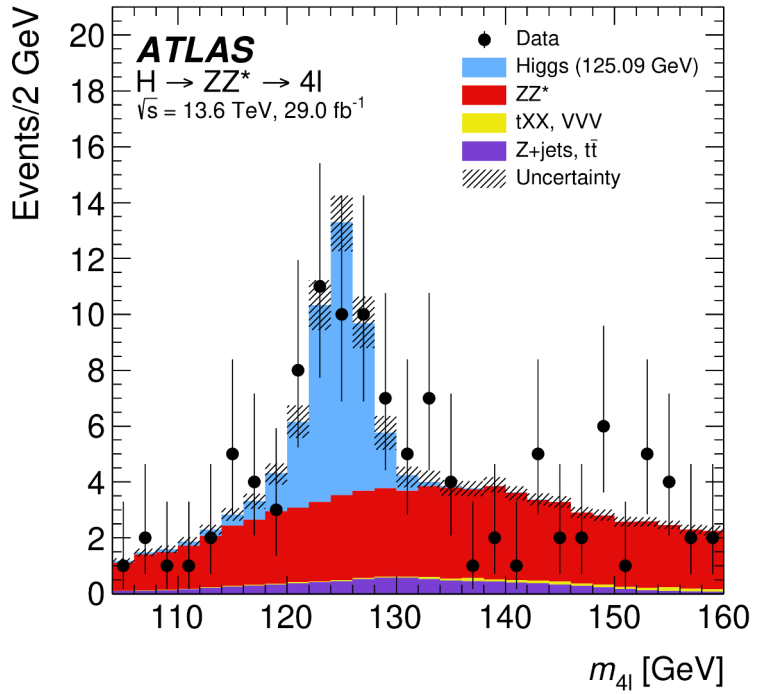

13.6 TeV Cross-Section Measurements

CMS 13.6 TeV $H \to ZZ^*$ and $H \to \gamma\gamma$ [HIGG-24-013 and HIG-23-014]

Aim:

- Measure fiducial and differential cross-sections in both channels separately.

Strategy:

- Similar to ATLAS: fiducial regions defined, fit to invariant mass spectra performed.
  - Addition for $H \to \gamma\gamma$: events separated into three categories based on mass resolution.

$H \to \gamma\gamma$

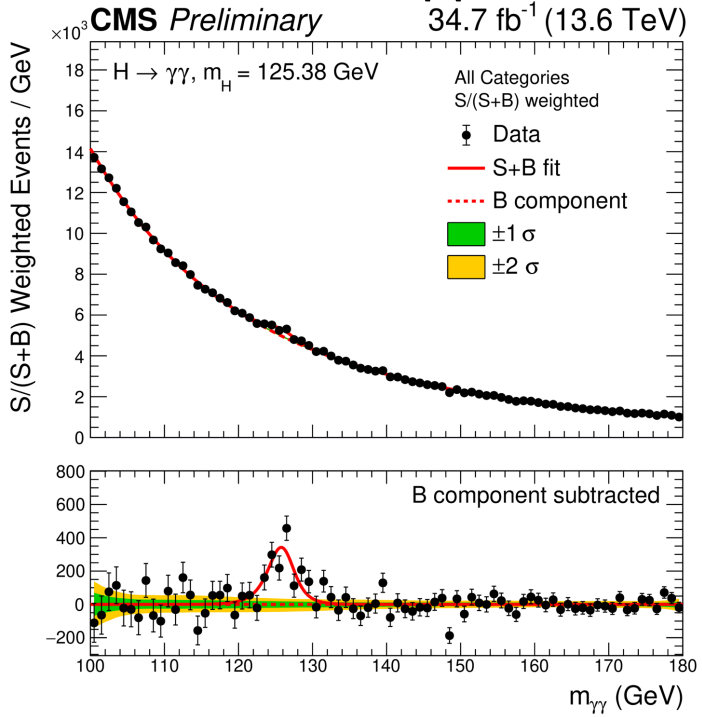

$H \to ZZ^*$

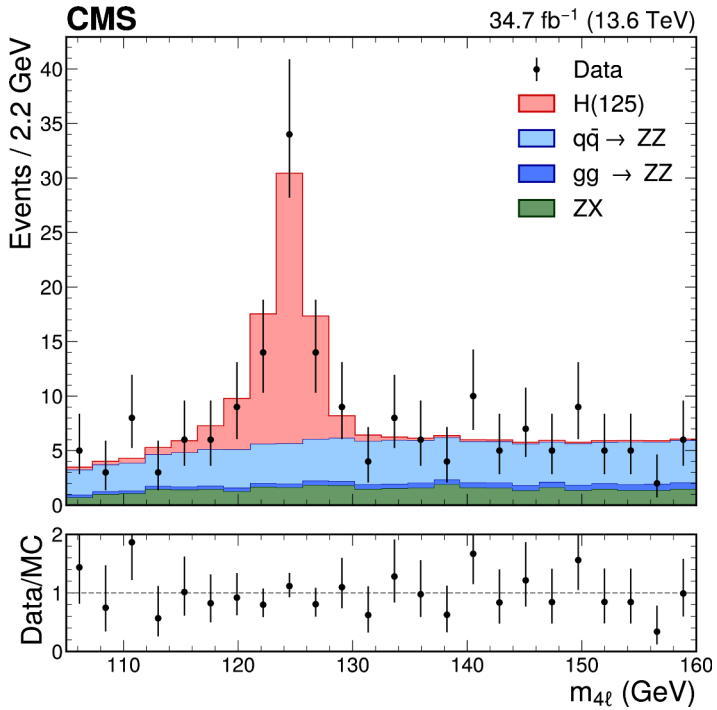

13.6 TeV Cross-Section Measurements

CMS 13.6 TeV $H \to ZZ^*$ and $H \to \gamma\gamma$ [HIGG-24-013 and HIG-23-014]

Strategy:

- Also split events into bins of p_{T}^{H}, $|y_H|$ and (for $H \to \gamma\gamma$) N_{jets}.

$H \to ZZ^*$

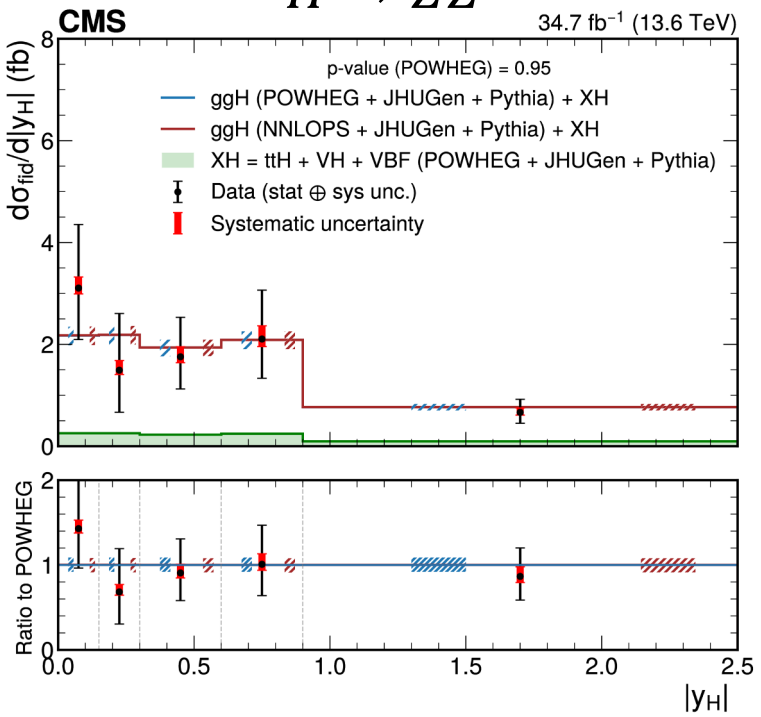

$H \to \gamma\gamma$

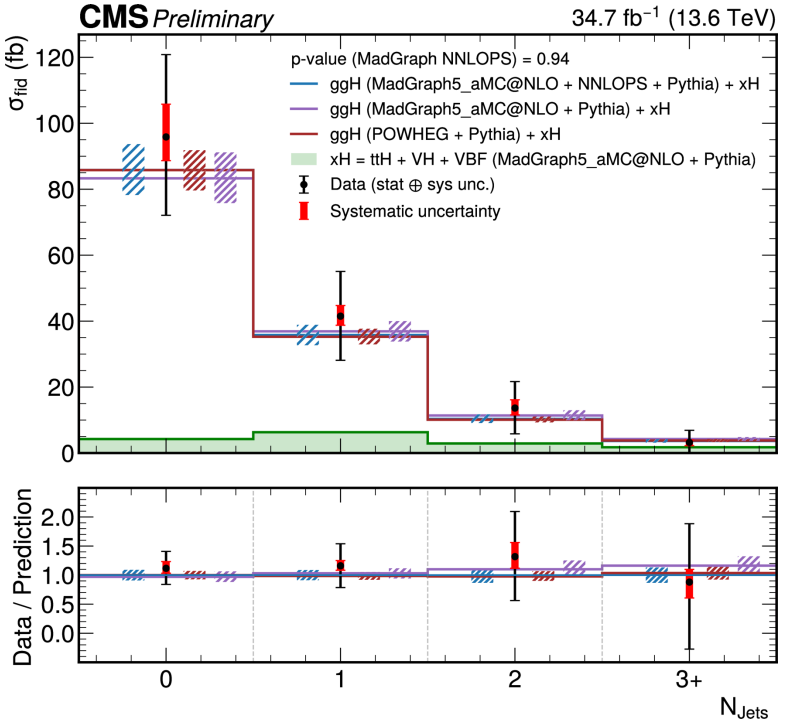

13.6 TeV Cross-Section Measurements

Results:

- Fiducial total and differential xsecs consistent with SM predictions.
- Results dominated by stat uncertainty.

CMS $H \rightarrow ZZ^*$

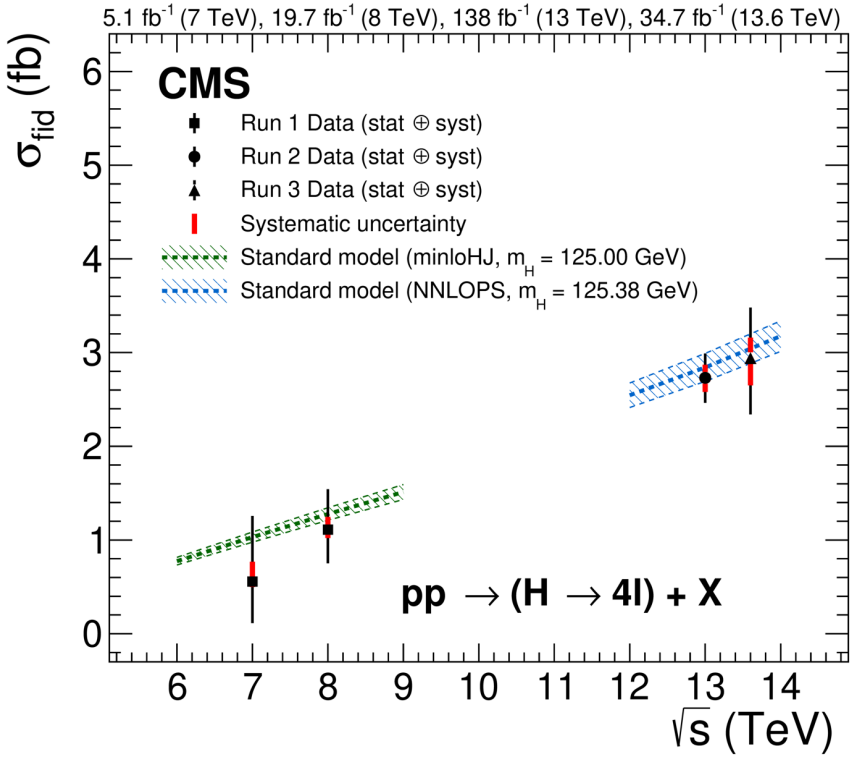

ATLAS $H \rightarrow ZZ^*$ and $H \rightarrow \gamma\gamma$